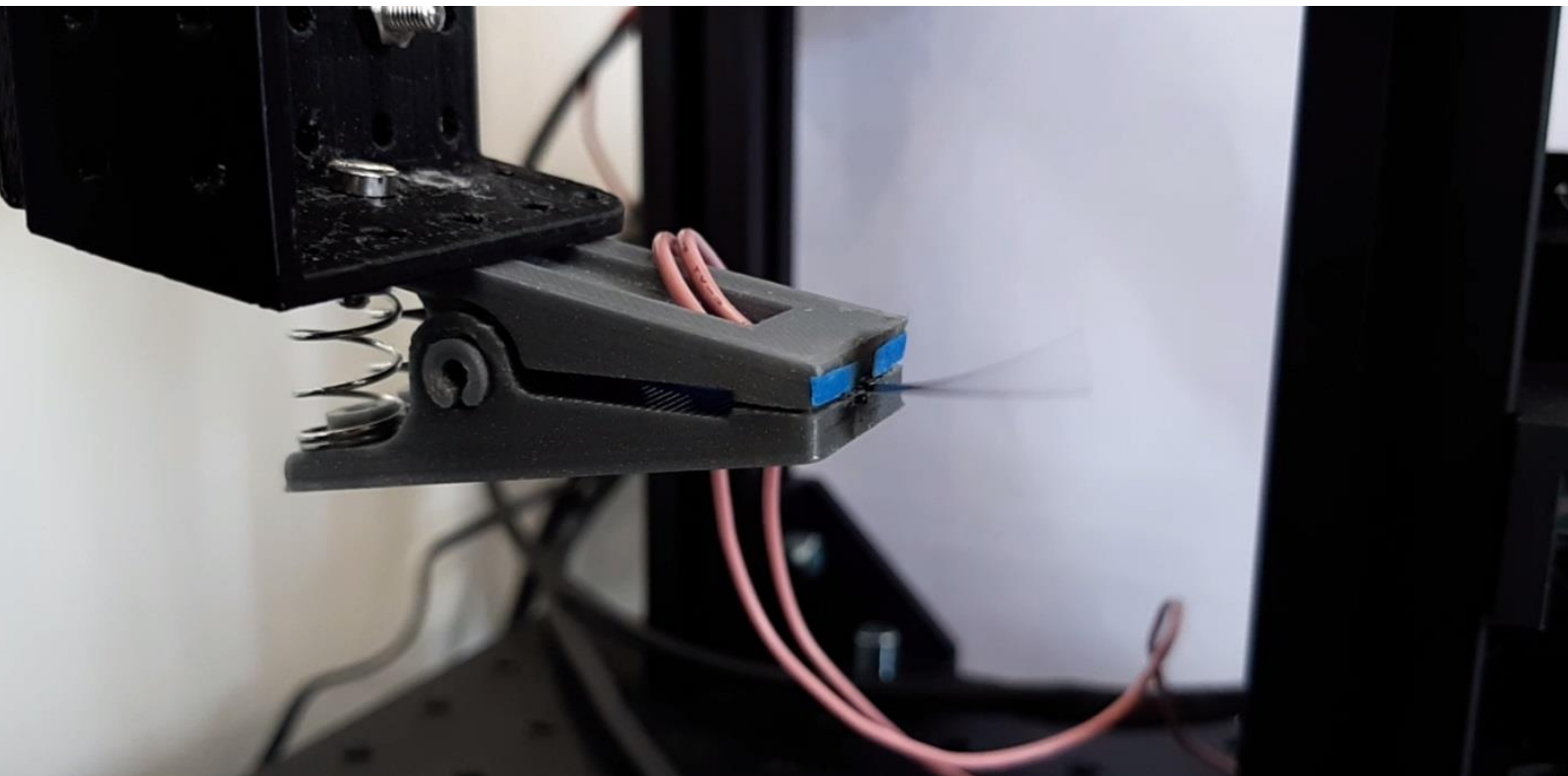


## Department of Precision and Microsystems Engineering

### **P(VDF-TrFE-CTFE) Actuators with Inkjet Printed Electrodes**

Koona-Garth Keith Baelz

Report no : 2019.024  
Coach : Andres Hunt, PhD; Hassan HosseinNia, PhD  
Professor : Prof. dr. ir. Just L. Herder  
Specialisation : MSD  
Type of report : Thesis  
Date : 17 July 2019





# P(VDF-TrFE-CTFE) Actuators with Inkjet Printed Electrodes

by

K. Keith Baelz

to obtain the degree of Master of Science  
at the Delft University of Technology,  
to be defended publicly on Wednesday July 17, 2019 at 2:00 PM.

Student number: 4731867  
Project duration: September 1, 2018 – July 17, 2019  
Thesis committee: Dr. A. Hunt, TU Delft, Daily Supervisor  
Dr. S. H. HosseinNia, TU Delft, Supervisor  
Prof. dr. ir. J. L. Herder, TU Delft, Chair  
Dr. M. K. Ghatkesar, TU Delft

*This thesis is confidential and cannot be made public until July 2021.*

An electronic version of this thesis is available at <http://repository.tudelft.nl/>.



# Contents

<b>I</b>	<b>Introduction</b>	<b>3</b>
<b>II</b>	<b>A Summary of Inkjet Printed Conductive Inks, Smart Materials, Sensors, and Actuators</b>	<b>5</b>
<b>III</b>	<b>P(VDF-TrFE-CTFE) Actuators with Inkjet Printed Electrodes</b>	<b>19</b>
<b>IV</b>	<b>Conductivity of Inkjet Printed Nanoparticle Dispersions on Polymer Substrates</b>	<b>27</b>
<b>V</b>	<b>Conclusions</b>	<b>37</b>
<b>VI</b>	<b>Reflections and Recommendations</b>	<b>39</b>
<b>A</b>	<b>Manufacturing Steps</b>	<b>41</b>
<b>B</b>	<b>Electrode Patterns</b>	<b>49</b>
	<b>Bibliography</b>	<b>53</b>



# Abstract

Inkjet printing offers an additive manufacturing method for the production of thin films. A variety of inkjet printed materials can be printed, including conductive and electroactive materials. Existing inkjet printed ferroelectric polymer actuators all utilize silver conductive layers and P(VDF-TrFE) for the electroactive layer. This thesis will describe the manufacture of P(VDF-TrFE-CTFE) actuators with inkjet printed carbon black electrodes. A conductive carbon black film is printed on a resin coated PET substrate to form the actuator bottom electrode. P(VDF-TrFE-CTFE) is spin coated on top of the electrode to form the active ferroelectric material, before finally another carbon black layer is printed on top to produce the top electrode. To validate the choice of electrode material, a selection of conductive inks are tested to compare conductivity and quality of deposition when printed with a commercial printer. The ease of printing and post processing is also compared to determine what ink can be used as an electrode material whilst requiring the fewest and quickest manufacturing steps. From this a model is produced to determine the maximum actuator operation frequency depending on electrode material. Produced actuators achieve  $206\ \mu\text{m}$  steady state deflections at 300 V and 3 mm at resonance. This shows an 89.4% improvement in strain per volt compared to similar inkjet manufactured P(VDF-TrFE) actuators in literature.







# Introduction

The advent of modern smart materials enable methods of sensing and actuation in new form factors, with greater strains and electromechanical performance than previously possible. Smart materials allow for the production of devices such as resonators, micropumps, and artificial muscles with compactness and strains not previously possible with traditional actuators. The manufacture of such devices however presents a significant challenge. Traditional methods of manufacture rely on masking or photolithographic methods which in addition to being both time intensive and costly, require special machinery to achieve [1]. As an alternative, inkjet printing can be used as a contactless additive manufacturing method to produce such devices. By suspending nanoparticles of conductive material inside a solvent, it is possible to inkjet print conductive traces. Other materials including electroactive polymers and piezoelectric ceramics can also be inkjet printed, allowing for the manufacture of completely inkjet printed ferroelectric and piezoelectric sensors and actuators. Whilst the existing inkjet printable materials are limited, it is expected that the research being done in this area will rapidly increase the types of materials that can be deposited using this method.

In order to render a solid inkjet printable, the solid material has to be reduced to a sufficiently small particle size and suspended in a solvent [2]. In order to print polymers, a suitable match of fluid viscosity and printing parameters have to be determined [3]. To form a foundation of what work has been done and what is possible, a literature study is presented on the existing inkjet printable conductive nanoparticle dispersions, and the inkjet printing of ferroelectric polymers. A comprehensive summary is provided on existing inkjet printed ferroelectric polymer devices, in addition to efforts done to print other active materials including piezoelectric ceramics and ionic electroactive polymers. Existing literature demonstrated the possibility to produce inkjet printed conductive films, as well as the suitability of inkjet printed electrodes for use with ferroelectric polymer actuators. Existing devices are however limited to inkjet printed silver electrodes and P(VDF-TrFE) polymer active layers [4, 5], or inkjet printed P(VDF-TrFE-CTFE) with sputtered Au electrodes [6]. It was determined that using carbon black electrodes in conjunction with P(VDF-TrFE-CTFE) could produce actuators with very simple manufacturing steps compared to manufacturing silver electrodes whilst still achieving greater deflections than reported in existing literature.

In the next section, the manufacturing methodology of a P(VDF-TrFE-CTFE) cantilever actuators with inkjet printed carbon black electrodes is described. The actuators are produced using a commercial printer to print the electrode layers, and spin coating to apply the polymer. The devices are extensively characterized, in both static deflection from a DC voltage as well as actuation from AC voltage across a frequency spectrum. The results demonstrate an increase in electromechanical strain compared to similar inkjet printed P(VDF-TrFE) actuators [4], and prove the viability of inkjet printed carbon black electrodes for use with ferroelectric polymer actuators. This paper was submitted to the ICCMA 2019 conference.

In order to compare the performance of different conductive inks and to gauge their po-

tential for use as electrodes, a series of inks were tested as part of the design process of the actuators. The results of this are included in a supplementary paper that describes the conductive performance of various materials of conductive nanoparticle inks across a range of polymer substrates. The quality of ink deposition as well as the effect of different post processing and sintering methods is evaluated to find what ink is best suited for use with thermally sensitive polymers, and what inks require the least post processing and can allow for the actuator to be manufactured with greatest ease.



# A Summary of Inkjet Printed Conductive Inks, Smart Materials, Sensors, and Actuators

The purpose of this paper is to provide the foundation and background for our research. This literature study describes the current state-of-the-art of various ferroelectric polymers, inkjet printing of conductive materials, and inkjet printing of active polymers and ceramics. The performance of different active materials and their ease of manufacture is evaluated, along with various conductive inks suitable for use as electrodes. Gaps in research are identified, along with promising electroactive polymers and electrode materials in order to determine the topic of our research.



# Inkjet Printed Sensors and Actuators - A Review of Inkjet Printed Conductive Inks and Smart Materials

K. Keith Baelz

**Abstract**—Ferroelectric polymers provide the possibility of electrostrictive and piezoelectric sensors and actuators with greater compliancy and strains than achievable with piezoelectric ceramic materials such as PZT. The manufacture of such devices is constrained by existing manufacturing techniques such as masking and photolithographic processes. Inkjet printing offers a promising additive manufacturing technique for producing thin films which could be utilized to this end. A review of existing printable materials and manufactured devices is provided to illustrate what is as of now possible, as well as what areas remain untouched. A number of fully inkjet printed ferroelectric polymer actuators were identified in literature, all using silver ink for their electrodes and P(VDF-TrFE) for the active layer. The use of carbon black instead of silver inkjet ink as an electrode material in conjunction with using P(VDF-TrFE-CTFE) as the active material has not yet been attempted, and could allow for the production of actuators with improved strain and ease of manufacture.

## I. INTRODUCTION

Traditional methods of manufacture for polymer actuators involve photolithographic methods, screen printed electrodes, spin coated polymers, or the use of pre-prepared polymer and electrode films that are then joined with adhesive. These methods generate material waste and can be time consuming whilst requiring special equipment. Inkjet printing has been extensively used to manufacture conductive traces used for wiring and circuitry using dispersions of conductive nanoparticles in a solvent. The possibility to print a wider range of materials including polymers and piezoelectric ceramics allows for the conception of fully inkjet printed sensors and actuators. Whilst some inkjet printed devices exist, the research in this field is limited in the choice of electrode material and type of polymer used. As such we propose the design and manufacture of a ferroelectric polymer actuator by inkjet printing using polymers with improved electromechanical strains and electrodes with lower stiffness, ease of manufacture and post processing. This paper first covers some fundamental information on ferroelectric polymers with examples of conventionally manufactured devices. A comprehensive overview of inkjet printable conductive inks is provided, followed by a summary of existing work towards the inkjet printing of polymers. Finally a compilation of existing sensor and actuator devices produced using inkjet printing is presented, categorizing the existing devices into ferroelectric polymer, piezoelectric ceramic, and other actuators. Through this we identify what conductive inks and ferroelectric polymers have been used to make actuators, what areas of research are lacking, and what existing conductive inks and electroactive polymers can be used to produce improved devices.

## II. FERROELECTRIC POLYMERS

Electro-active polymers (EAPs) are polymers which exhibit a change in shape in response to electrical stimuli [1]. EAPs can be split into 2 classes, ionic and electronic polymers [2]. Ionic EAPs function based on the transport of ions inside the material. Though ionic EAPs can function with lower voltage than electronic polymers, they also exhibit lower forces [3], lower bandwidth [4], and must be operated in a solvent or contain ionic liquids [3]. Electronic EAPs function through electrostatic forces, such as electrostatic, piezoelectric and ferroelectric effects. Whilst electronic EAPs require much higher driving voltage, they can actuate rapidly with a millisecond response rate, and maintain a constant deflection when subjected to a DC voltage source [2]. This report will focus on electronic EAPs, specifically ferroelectric polymers.

Ferroelectricity describes the characteristic of a material, where a spontaneous electric field is present. These materials will maintain a constant electric field, although this field can be neutralized or reversed through an external electric field [5]. Ferroelectricity is a subset of pyroelectricity, a property of materials in which they are able to produce a voltage in response to temperature change. In addition to this, ferroelectric materials are also inherently piezoelectric, meaning they accumulate charge in response to pressure or mechanical deformation. The piezoelectric effect is reversible, in which an applied charge will produce a mechanical strain in the material [6]. All these properties allow ferroelectric materials to be used as transducers used to sense thermal changes or to convert charge into deflection, making them particularly useful in sensing and actuation.

The most common ferroelectric polymer is PVDF, possessing high mechanical strength and good chemical resistance. PVDF can exhibit electrostrictive strains of around 2% [2]. PVDF can be manufactured using extrusion, machining and injection or compression molding, making it useful in a wide spectrum of applications. The inclusion of a TrFE monomer into this polymer produces P(VDF-TrFE), granting improved electromechanical properties. The inclusion of the monomer increases the volume of the unit cell and separates the VDF monomers, reducing the interaction of dipoles between the monomers. This grants increased mechanical strain as a result of electrical input and allows for greater sensitivity when used in transducers [7]. The improved strain characteristics make this polymer suitable for producing actuators where larger deflections are desired.

The addition of a comparatively large chlorine atom into the

polymer structure imposes a large steric hindrance, limiting the repulsion forced between the hydrogen and fluorine atoms. As a result of this, higher polarization is achieved by the dipoles of all monomer pairs, improving electromechanical performance [8]. This produces P(VDF-TrFE-CTFE), a relaxor ferroelectric polymer and eliminates dielectric heating and poling hysteresis. Relaxor ferroelectrics exhibit extremely high electrostriction in addition to high dielectric constants. P(VDF-TrFE-CTFE) can exhibit electromechanical strains greater than 5% and possesses a high breakdown voltage, making it particularly suitable for thin flexible actuators [8].

The manufacture of devices from ferroelectric polymers is traditionally done using pre-prepared films that are then attached to electrodes through an adhesive. Perez et al. produced a bimorph cantilever PVDF actuator using commercially available PVDF films with Ni/Cu electrodes, as well as coating non electrode films using a metal evaporator [9]. The produced 20 mm long cantilever actuators achieved a maximum deflection of 21.55  $\mu\text{m}$  with 40 V DC. In this example both layers of the bimorph are connected in series and used for actuation.

Engel et al. produced a bimorph cantilever actuator using a layer of P(VDF-TrFE-CTFE) film for actuation and a layer of PVDF film for sensing [10]. The PVDF film used consisted of commercially available sheets cut to size, whilst the P(VDF-TrFE-CTFE) polymer was applied through spin coating. The electrodes for the PVDF layer consisted of commercially available silver film, whilst the electrodes for the P(VDF-TrFE-CTFE) consisted of sputter coated gold. The produced 6.5 mm long cantilever actuators achieved a maximum deflection of 350  $\mu\text{m}$  when operating at a resonance frequency of 525 Hz excited at peak to peak 300 V AC.

Both the electrodes and active polymer layer of ferroelectric polymer devices can be manufactured through a number of different techniques depending on the necessary specifications. A notable method that is rising to prominence is printing. Printing covers a large range of techniques including screen printing, flexography, rotogravure and more. Such methods offer a way to simply and rapidly deposit a fluid on choice on a substrate in the desired pattern. Whilst traditionally used with simple colored ink, an expanding range of active materials in printable mediums has allowed for printing to be utilized in part or in full for the manufacture of active devices.

### III. INKJET PRINTING FOR MANUFACTURING

The deposition of material on a substrate through printing can be divided into 2 classes. The first class consists of manufacturing methods dependent on stencils, mask-based, and photolithographic processes. Included in this are screen printing, and printed circuit boards. The second class consists of additive manufacturing methods, most commonly inkjet printing [11]. Inkjet printing offers a contact free method for depositing a wide range of fluids and materials onto a substrate at ambient temperature and pressure [12]. Inkjet printing allows the precise deposition of picoliter volume of material in desired patterns without the need for masks. Through this, the total number of manufacturing and processing steps

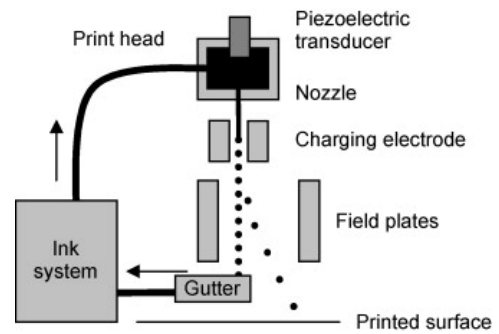


Fig. 1. Operating principle of CIJ inkjet printing [14]

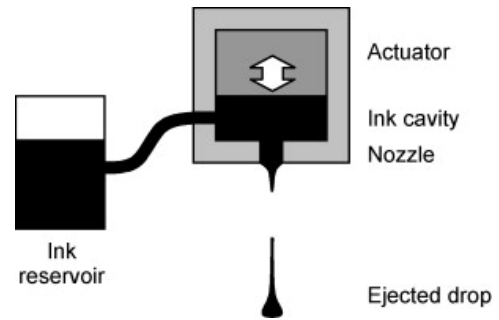


Fig. 2. Operating principle of DoD inkjet printing [14]

is reduced compared to masking processes, along with the amount of time and of space required for manufacture, and the waste generated [13]. Inkjet printing can be further subdivided into 2 categories, continuous inkjet (CIJ) and drop on demand inkjet (DoD).

#### A. Continuous inkjet printing

In CIJ printing, a continuous stream of fluid is excited through the use of a piezoelectric transducer in order to break surface tension and form a stream of droplets. The droplets are then steered electrostatically to the desired position on the substrate with an electric field (Fig. 1). Any droplets that are not deflected and used for printing are recirculated and reused [14].

#### B. Drop on demand inkjet printing

In DoD printing, there is no need for a continuous stream of fluid or recirculation, and fluid is only deposited when needed. The fluid is ejected from a reservoir out of the printing nozzle by means of a pressure pulse (Fig. 2). This pulse is commonly generated in 2 ways.

Thermal DoD printing uses a small heating element located near the printing nozzle to heat the fluid very briefly into a vapor state. This sudden expansion drives the fluid out of the nozzle. As the vapor bubble cools and collapses, it draws ink from the reservoir to restore the cavity. Due to the process of vaporization, this method of printing is not suitable for use with all materials and requires inks to have a volatile component [14].

Piezoelectric DoD uses a piezoceramic plate that alters its thickness with respect to an input voltage and induces a pressure wave into the fluid forcing a droplet out of the nozzle. The excitation of the piezoceramic plate is governed by a waveform which determines the voltage rising time, dwell time, and falling time. In order to achieve droplet ejection, it is necessary to find the correct parameters for applied voltage and duration of the pulse. Both these parameters have a heavy influence on droplet size and formation [13]. As piezoelectric DoD does not alter the printed fluid in any way, it is not subject to the same limitations in printable fluids as thermal DoD is.

DoD printing offers higher resolutions and produces less waste than CIJ, making it more suitable for microelectronics manufacturing [12]. Industrial inkjet printers remain costly due to the need to be compatible with a wide range of inks, including metal based and polymeric inks. Office inkjet printers commonly function commonly using thermal DoD, although some brands with piezoelectric printheads can be found (Epson and Brother Co.) [15]. Office printers suffer from incompatibility with functional inks due to high viscosity and nozzle occlusion issues, though there is a rise in the prevalence of conductive inks suitable for use with office printers, allowing for the production of simple devices [11].

#### IV. INKJET PRINTING CONDUCTIVE INKS

The most common functional inkjet ink commercially available and the most frequently mentioned in existing literature is conductive ink. Printable conductive inks are composed of conductive particles suspended in a fluid. These colloids consist of nano-particles of conductive material dispersed in a carrier fluid, typically a solvent. The specific use of nanoparticles in these inks rather than larger particles is vital as particle sizes under 50 nm in diameter help to prevent sedimentation or aggregation that would otherwise occur with larger particle sizes [16]. The solid material to solvent ratio has to be selected carefully in order to maintain a viscosity that still allows for printing. Higher solid content will raise the viscosity and increase the risk of clogging printhead nozzles but will offer higher conductivity. Different piezoelectric printheads will be capable of printing different fluid viscosities and as such inks have to be chosen that contain high enough solid content to achieve the desired conductivity whilst still allowing for consistent printing.

##### A. Silver nanoparticle inks

Silver nanoparticle inks are by far the most common ink used throughout literature, for everything from simple circuits such as the RFID antennae shown in Fig. 3 to more complex actuator devices. In its simplest form, silver inks consist purely of silver particles in a solvent, with a solid weighting commonly ranging from 15-55% [17, 16]. Lower weightings from 15-25% are appropriate for use with conventional office printers [18], whilst higher silver content inks are intended specifically for industrial grade inkjet printers such as the Dimatix or Jetlab series printers [19]. These inks can be

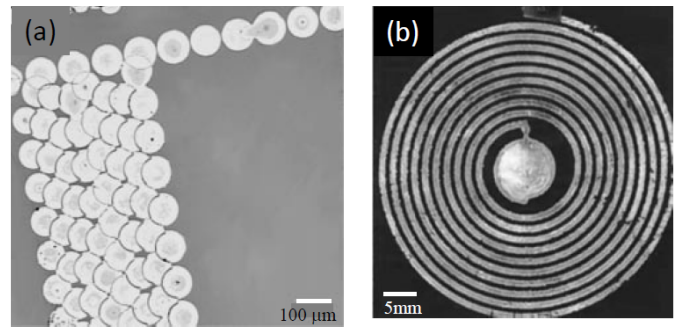


Fig. 3. Inkjet printed silver nanoparticle ink (a) printed ink droplets; (b) printed RFID coil [16]

printed onto to a wide variety of substrates and will adhere, but will not achieve conductivity on most substrates until sintering.

1) *Thermal sintering*: Heating the printed patterns is typically sufficient to dry the solvent and sinter the silver nanoparticles together to produce conductivity. The required sintering temperature is highly dependent on the particle size, and the smaller the particle size the lower the sintering temperature. As a result, newer optimized inks can achieve as high as 70% the bulk conductivity of silver whilst sintering at 150 °C [20], whilst previously silver inks could only achieve 20-30% bulk conductivity under the same sintering conditions [18, 15, 21].

Whilst the temperatures required to sinter some more specialized inks can be as low as 120 °C [22], not all substrates will survive being heated to these temperature, especially thin polymer films. Inks capable of being sintered at such low temperatures are at this point are a relatively recent development and remain fairly uncommon. As a result the inks available come in few formulations which are typically only usable with industrial grade printers. There are a number of alternative approaches that can be employed to instead sinter the printed silver particles without heating up the substrate rather than depending on the curing temperature of the ink itself.

2) *Photonic sintering*: The most common alternative to thermal sintering is photonic sintering, in which printed conductive inks are exposed to a light source of sufficient intensity to melt and join the nanoparticles. This method is specifically suitable for nanoscale materials due to the phenomenon of melting-point depression. The increased surface area to volume ratio as well as different absorption spectra of nanoparticles allows nanoparticles to melt at temperatures several hundred degrees lower than identical bulk material [23]. Photonic sintering is most typically performed using either intense pulsed light (IPL) or a laser as a light source.

IPL uses a short pulse of light typically from a xenon flash bulb to heat the conductive nanoparticles to their melting point. Xenon flash lamps produce a broad spectrum of light ranging from UV to IR (Fig. 4), whilst a laser light source will only produce light in a specific narrow band of wavelength. Certain materials of conductive inks such as copper require certain wavelengths of light to be sintered, and only a laser source

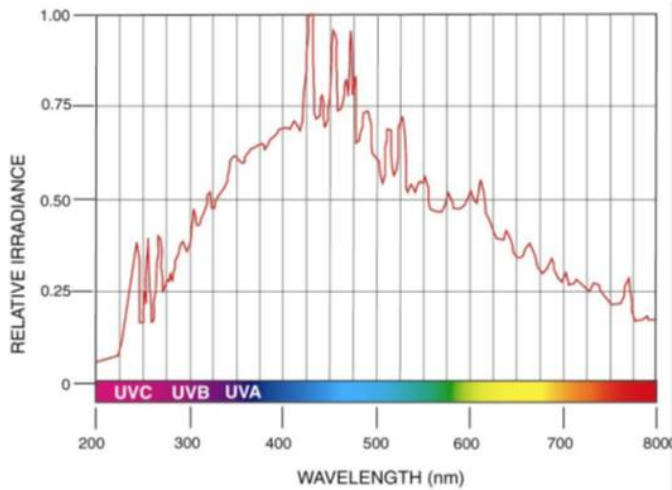


Fig. 4. Wavelength spectrum emitted by a Xenon bulb [23]

with the corresponding wavelength will be able to sinter the inks and produce conductivity. Due to the broad spectrum of light produced through IPL, there are no such concerns. IPL also possesses a number of additional advantages of laser sintering. Emitting IPL in brief pulses allows a higher peak power to be emitted compared to continuous emission, and heats up a thin film of material to an extremely high temperature. Due to the pulse of light being applied very briefly, the heat is can be rapidly dissipated into the substrate via conduction. As the heating effect is extremely intense but also very brief, it is able to effectively sinter conductive particles at extremely high temperatures whilst avoiding any damage to the underlying substrate [24]. Several pulses can be emitted with intermittent cooling periods, and full sintering of conductive inks can be achieved near instantaneously.

3) *Chemical sintering*: Significantly less common are chemically sintering inks. These inks are a departure from the simple 2 component inks of purely nanoparticles in solvent, and are instead formulated to give rise to conductivity once exposed to the appropriate reagent.

Pabst et al [21] found that sintering a 55% wt silver ink in a low pressure argon plasma chamber was able to sinter the silver particles without damaging the underlying substrate. The resultant conductivity was 20-30% of bulk, and would otherwise have required thermal sintering at 150 °C. Whilst effective, this approach requires fairly specialized equipment, and does not produce conductivities any higher than thermal sintering.

It is possible to produce a self sintering silver ink by mixing silver nanoparticles with a diameter of less than 0.1  $\mu\text{m}$  in a polymer latex and halide emulsion. The polymer latex in combination with the silver nanoparticles form an interconnected structure, which is accelerated by the halide. These structures are then stabilized through the introduction of water [25]. Once printed, conductivity appears seconds after drying, through conductivity can be improved through

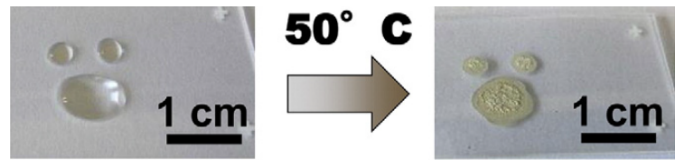


Fig. 5. The transition from the complexed silver ink to metallic silver after heating at 50 °C. [26]

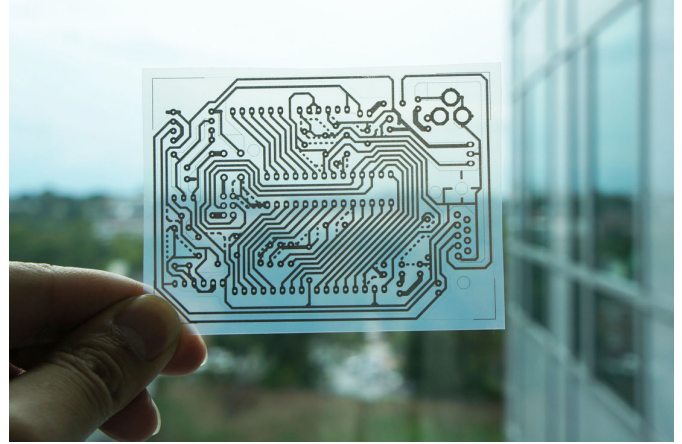


Fig. 6. PCB printed using self sintering silver inkjet ink [25].

exposure to moisture. The conductivity is however highly dependent on the substrates on which the silver ink is deposited. Best conductivity is achieved when printed on porous substrates such as resin coated PET films or photo ink on which achievable sheet resistance values range from 0.19  $\Omega/\square$  to 0.28  $\Omega/\square$ . On certain substrates, the sheet resistance will remain in the excess of 100  $k\Omega/\square$  indicating this ink is suitable only for certain applications [15]. An example of a PCB printed with this ink is shown in Fig. 6.

An alternative approach is to produce an ink containing silver in the form of a dissolved complex rather than solid nanoparticles [26]. After heating at 50 °C all reactants are evaporated, leaving only pure silver behind (Fig. 5). Such an ink solution can consist of a mixture of silver acetate and ammonium hydroxide in its simplest form, though this formulation leads to clogging as silver particles form at the printer nozzles after a few minutes of printing. An improved formation is suggested wherein ammonium hydroxide is substituted for propyl amine, before titrating with formic acid to filter out any metallic silver still present before printing. The propyl amine possesses a higher boiling point and reduces the speed of evaporation, thus reducing the clogging at the nozzle tips. Using this formulation, the conductivity achievable when printing on glass is 14 times lower than bulk silver.

### B. Copper nanoparticle inks

A less common alternative to silver inks are copper nanoparticle inks. Though copper inks have the benefit of relative affordability compared to silver inks, they require more intensive post processing steps. In addition to this, their comparative



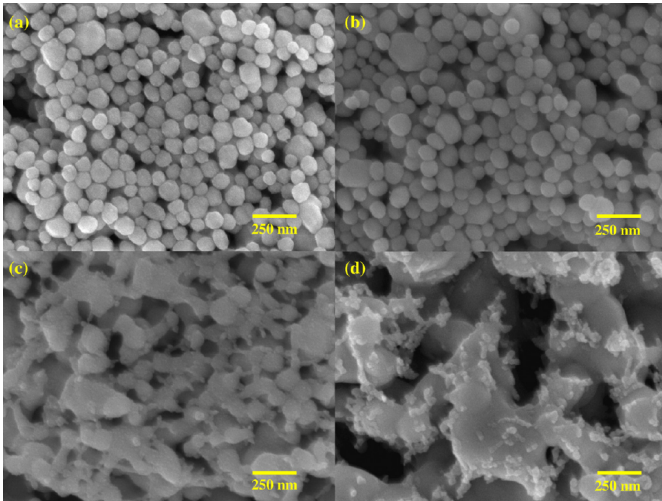


Fig. 7. SEM images showing the microstructural evolution of the granular conductive patterns in copper nanoparticle ink as a function of annealing temperatures: (a) 200 °C, (b) 250 °C, (c) 300 °C, and (d) 350 °C. The samples were heat-treated on a hot plate at each temperature in vacuum for 1 h [28].

rarity to silver inks means there are no chemical or self sintering inks available, and the vast majority of commercially available inks are reliant on photonic sintering. Due to the high reactivity of copper, the oxidation rate increases exponentially with respect to increasing temperature in an ambient environment [27]. Copper will very easily become oxidized into Cu<sub>2</sub>O or CuO, both of which possess reduced conductivity compared to copper [28]. In order to achieve conductivity of printed copper patterns, there are a number of methods. The copper oxide nanoparticles have to either be converted back into Cu, a protective coating can be applied to the Cu particles to prevent oxidation before sintering [29], or the sintering process can be performed inside an inert environment [27].

1) *Thermal sintering*: Thermal sintering of copper particles is possible, though it requires very high temperatures which are non compatible with polymer substrates [30]. By using Polyvinyl-pyrrolidone (PVP) as a capping molecule, Cu particles can be produced with a PVP coating at the surface to protect the copper from oxidation. These particles show stability with no oxidation after being stored at ambient conditions for 30 days. During thermal sintering, the resistivity of printed regions decreases with increasing sintering temperature. Sintering below 200 °C shows no change in particle composition, whilst heating above 250 °C causes a very rapid decrease in resistivity. At temperatures past 325 °C, there is no noticeable improvement in conductivity. The best conductivity was achieved when heating at 325 °C for 1hr, resulting in conductive films with 10% of bulk material conductivity [28]. The effects of thermal sintering are shown in Fig. 7.

2) *Photonic sintering*: Copper ink can be sintered through IPL or with a laser, in which the intense brief burst of energy is enough to sinter the particles, but not long enough to allow

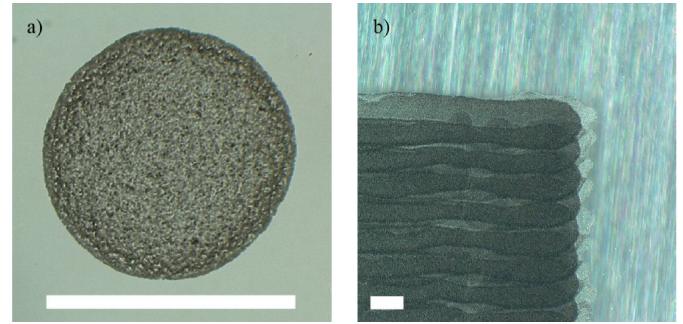


Fig. 8. a) Bright field digital microscope image of a droplet of carbon black ink printed on an Elastosil membrane. The length of the scale bar is 125µm. b) Dark field image of an array of carbon black ink printed with a horizontal and vertical droplet spacing of 50µm. [33]

the copper to oxidate. A limitation in laser sintering is that the laser source be in the 808-1064 nm wavelength [31]. Low scanning speeds when sintering using a laser will heat the printed copper nanoparticles enough to cause oxidation and reduce conductivity. Increasing the scanning speed so that the laser only shines on an area of copper very briefly can allow for the copper to be sufficiently sintered without heating it up enough to cause oxidation, but there is a threshold after which increasing scanning speed will also lead to increasing sheet resistance. As such the individual parameters have to be selected carefully to optimize conductivity [27]. A broad spectrum light source as used in IPL does not face this same issue in wavelength as a laser source, and can sinter a large area at once compared to the small spot size of a laser source. In IPL, the energy density, bank voltage, power duration as well as number of pulses and time between pulses can all be varied to obtain ideal sintering parameters. IPL sintering also tends to produce better conductivity than laser sintering, achieving up to 20% of bulk conductivity whilst laser sintering achieved up to 16% [30].

### C. Carbon inks

Carbon inks offer a unique alternative to metal nanoparticle inks altogether in that they typically do not require any form of sintering to become conductive. Whilst carbon inks typically possess much lower conductivity than metal inks, they have the advantage of high compliance and do not add to the effective stiffness of dielectric elastomer actuators (DEA) [32]. Carbon black electrodes can come in several forms, including carbon black nanoparticles, carbon nanotubes, and graphene.

1) *Carbon black nanoparticle inks*: Traditional carbon black electrodes consist of carbon grease electrodes, wherein carbon black powder is combined with silicon oil and the resultant paste is applied manually. The issues associated with such electrode greases are their poor adhesion, leading to poor robustness [32].

In comparison to this, conductive carbon black inkjet ink consists of 3 parts, carbon black powder, a dispersant (Belsil SPG 128 VP, Wacker Chemie AG), and a solvent (OS-2, Dow Corning). This ink shows good resistance to mechanical wear

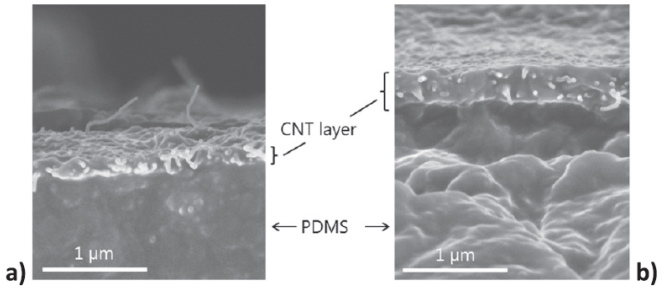


Fig. 9. SEM images of two different inkjet printed CNT-layers. (a) Cross-section view of a thin (<100 nm) CNT-layer and (b) cross-section view of a thick CNT-layer (200 nm) [37].

and shows no degradation when submitted to large strains over several cycles. When a single layer of this ink is printed, a conductivity of  $30 \text{ k}\Omega/\square$  is achievable, and with 2 layers the resistance drops to  $13 \text{ k}\Omega/\square$  [33]. A printed sample of this ink is shown in Fig. 8. When used with silicone based DEAs, inkjet printed carbon electrodes show greatly improved reliability and robustness when compared to manually applied carbon grease electrodes which suffer from poor lifetimes [32].

2) *Carbon nanotubes*: Carbon nanotubes (CNT) promise improved conductivity whilst still having low material cost, though face significant difficulties when used in inkjet printing. CNTs exhibit hydrophobicity in addition to strong Van der Waals interactions, causing them to agglomerate which can lead to nozzle clogging and unreliable printing. To circumvent this, a number of methods are available such as the use of specific organic solvents [34], the inclusion of surfactants in water based inks [35], or covalent side wall functionalisation [36]. A number of drawbacks exist for each method. The organic solvents suitable for this application pose a health and environmental risk, and the defects introduced through side wall functionalisation reduce the conductivity of CNTs. The use of water based inks may not be possible with all printers, as some printers require inks with low surface tension to be able to print. Water based inks may also require anti foaming agents which reduce the conductivity.

To circumvent these shortcomings, a possible solution is to use multiwall CNTs in a mixture of 95% organic solvents and 5% water, where the organic solvent maintains the low surface tension required for printing, and a water/surfactant blend keeps the particles well dispersed [37]. This ink blend was able to produce layers with a sheet resistance of  $6\text{-}7 \text{ k}\Omega/\square$ , notably outperforming the conductivities achievable with carbon black inks. A cross sectional view of inkjet printed layers of this ink are shown in Fig. 9.

3) *Graphene*: Graphene possesses the advantages of high mechanical strength and flexibility in addition to high conductivity and transparency, although they require some post processing in contrast to other carbon based conductive inks which require none. To produce an inkjet printable ink, graphene oxide (GO) is first synthesized from natural graphite using a modified Hummers and Offeman method, before exfoliating in water and washed for 4 cycles of centrifugation

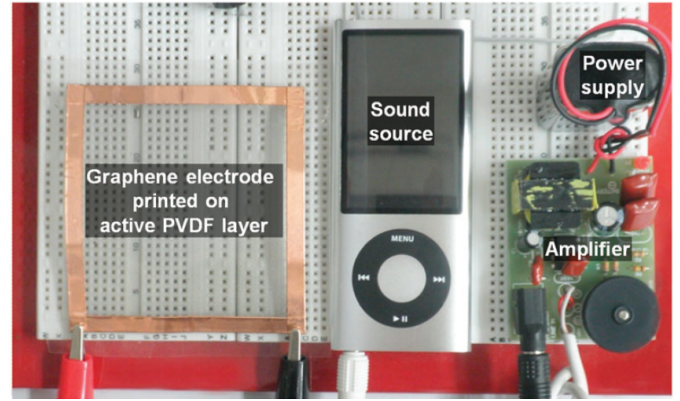


Fig. 10. PVDF-based thin film acoustic actuator using flexible and transparent graphene electrode [38].

to remove remnant unexfoliated GO. This resultant GO is then suspended in distilled water to produce the inkjettable ink. Once the aqueous graphene oxide is printed, the printed layer is thermally sintered under vacuum conditions to reduce it back into graphene. The resultant thin film consists of multiple layers of graphene, and can achieve a sheet resistance of  $1.5 \text{ k}\Omega/\square$  at 180 nm film thickness [38]. An example of an acoustic actuator produced using this ink is shown in Fig. 10. Whilst ready made graphene ink is also commercially available, it remains prohibitively expensive and requires curing temperatures from  $250\text{-}300 \text{ }^\circ\text{C}$  (Graphene ink 793663, Sigma Aldrich).

## V. INKJET PRINTING POLYMERS

The deposition of polymer is typically achieved using spin coating or dip coating. The limitations of this method are that in order to apply polymer only to specific regions, photolithographic methods have to be employed, increasing the production cost, manufacturing time, and waste involved. Inkjet printing offers a way to selectively deposit polymer on a substrate. Polymer inks however possess non-Newtonian rheological properties, complicating the printing of such inks.

### A. Viscoelasticity of polymer inks

When subjected to a shear flow at very low and high shear rates, polymer solutions tend to exhibit a shear thinning effect, effectively reducing the viscosity of the solution for as long as it is subjected to the shear strain. However, during inkjet printing the droplets of polymer are forced at a high speed through a very small orifice. Through this process, the polymer solutions are subjected to a significant elongational deformation, leading to greater stretching and orientation of the polymer macromolecules than would occur in ordinary shear flow. High molecular weight polymer solutions have the tendency to form a strong resistance to elongational deformation, yielding an increase in longitudinal viscosity. This resultant viscoelasticity present in non-Newtonian fluids can prevent ink droplets from detaching from the printing nozzles, leading to inconsistent ink flow during printing. As the ink

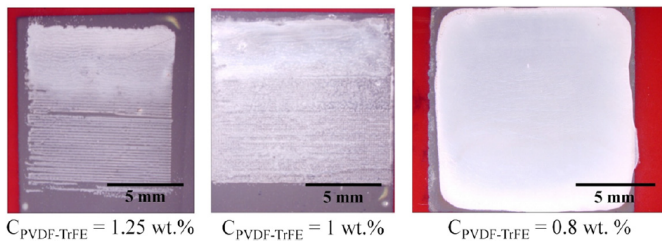


Fig. 11. The effect of different amounts of polymer material on printability [12].

droplet that flows out of the nozzle experiences stretching in the polymer macromolecules, a restoring force causes the droplet to decelerate before eventually reversing its direction and returning to the nozzle. This can be circumvented through the increase in droplet velocity once the ligament attaching the droplet to the nozzle is fully stretched and about to break. Thus the printing of high viscosity polymeric inks require significant optimization of the printing parameters, and require the voltage waveform by which the piezoelectric printhead is excited to be adapted for the rheological behavior of the polymer ink [12]. The effect the addition of polymer has on inkjet printing inks is shown in Fig. 11.

When printing polymer inks, the polymer structure, molecular weight, and concentration all have an effect on the macromolecular stretching behavior. The mechanism of polymer chain behavior in inkjet printing remains not fully understood, and the information on appropriate printhead waveforms with regards to rheological properties remains lacking [39].

### B. Coffee stain effect

When a droplet of dispersion or solution dries on a smooth substrate, the remaining material dries in an uneven pattern, forming a thicker ring around the edge of the droplet and hindering even deposition. An example of this is shown in Fig. 12. This occurs due to pinned position of the boundary between the edge of the droplet and the substrate, as well as the increased evaporation rate at the edge of the droplet. When an evaporating solvent particle escapes the surface of the droplet near the center, the random walk of the particle gives it a higher chance to find its way back into the droplet and become reabsorbed. Evaporating solvent particles near the edge of the droplet have a much lower chance of reabsorption, and as such have a higher rate of evaporation [13].

This phenomenon can be avoided in a number of ways. Using a solvent mixture consisting of a solvent with a low boiling temperature and high vapor pressure in conjunction with a solvent with high boiling temperature and low vapor pressure has been shown to completely eliminate coffee stain behavior in inkjet printed P(VDF-TrFE) microdots [40]. Printing on a cooled substrate has also been shown effective in eliminating the coffee stain effect in inkjet printing PEDOT:PSS droplets [41]. When even film deposition is required, it is necessary to keep this phenomenon in mind and formulate the polymer ink accordingly.

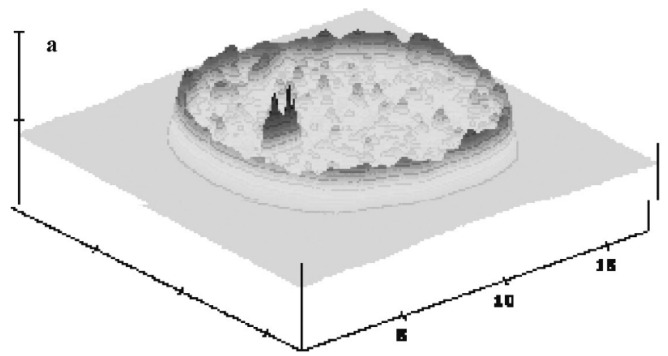


Fig. 12. AFM images of P(VDF-TrFE) microdot printed from DMF solution exhibiting the coffee stain effect [40].

## VI. INKJET PRINTED DEVICES

Through the inkjet printing of conductive inks, it is possible to print the wiring, contacts, or electrodes of actuators. Inkjet printing can also be used to deposit the active material of the device onto the electrode in the desired pattern. Inkjet printing may be suitable for printing both the electrodes and active materials in certain actuator types, opening up the possibility for fully inkjet printed devices. The numerous types of actuators produced either by part or fully through inkjet printing that appear in literature can be categorized based on their active material.

### A. Ferroelectric polymer devices

The majority of ferroelectric polymer actuators appearing in literature are based on Polyvinylidene fluoride (PVDF) and copolymer polyvinylidene fluoridetrifluoroethylene P(VDF-TrFE).

Zhang et al. showed that the printing of P(VDF-TrFE) could be achieved by dissolving the polymer in Dimethylformamide (DMF), though this formulation produced coffee ring patterns when the droplets dried. To rectify this, a mixture of low boiling temperature and high vapor pressure (DMF) solvent together with a high boiling temperature and low vapor pressure solvent (dioctyl phthalate) was able to completely eliminate coffee ring effects [40].

A number of fully inkjet printed P(VDF-TrFE) sensors and actuators are reported. Oliver et al. produced an all inkjet printed P(VDF-TrFE) membrane for use in a micropump, as well as cantilever actuators [21]. The actuator was based on a PET substrate on which silver nanoparticle ink was printed, before being sintered through low pressure argon plasma exposure. The polymer ink was then printed on top, and sintered at 130 °C. The final top electrode is then printed on the polymer and sintered using the same process as the bottom electrode. The finished cantilever actuator and micropump are shown in Fig. 13. The silver ink selected for this application did not possess a low enough sintering temperature to be used on PET, and as such argon plasma sintering was employed to reduce the temperature required to achieve conductivity in the

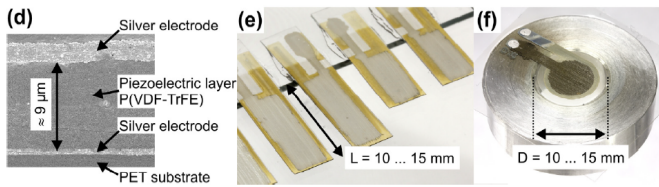


Fig. 13. (d) Cross-sectional SEM image of actuator structure. Cantilever (e) and membrane samples (f) mounted on glass and aluminum mounts for characterization. [21]

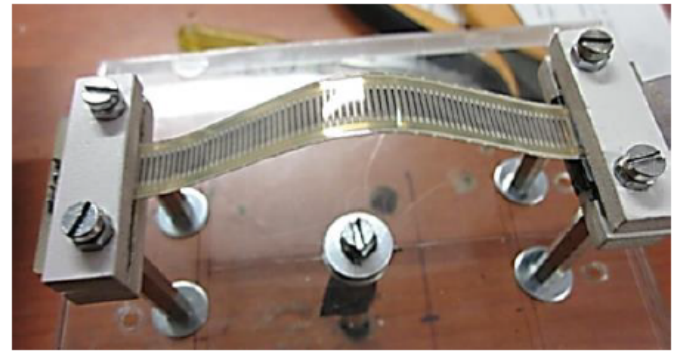


Fig. 14. Inkjet printed bistable PZT actuator [45].

electrode layer. The polymer ink consisted of polymer powder dissolved solely in cyclopentanone.

Thau et al. produced all inkjet printed piezoelectric transducer using P(VDF-TrFE) in combination with printed silver nanoparticle electrodes using slightly different materials and methods [42]. By formulating a polymer ink using a combination of solvents (cyclopentanone/DMSO), they demonstrated an optimized polymer ink formulation which produced consistent and repeatable printing. The actuator was based on a PEN substrate on which a silver nanoparticle ink was printed, before being thermally sintered at 100 °C. The polymer ink was then printed on top, and sintered at 140 °C. The final top electrode is then printed on the polymer and sintered at 100 °C. The use of a silver ink with low sintering temperature (Genesinks) allowed the actuator to be produced using a polymer substrate, without requiring any special post processing steps. The resultant P(VDF-TrFE) thin film exhibited piezoelectric and ferroelectric properties comparable with those exhibited by spin coated thin films.

In contrast to fully inkjet printed actuators, Shin et al. Produced an acoustic actuator from graphene conductive ink using a pre prepared PVDF film substrate [38]. In this application, the aqueous graphene electrode ink is printed directly onto the PVDF film, eliminating the need for a separate substrate. This also reduces the number of printing operations and inks required. The use of graphene ink shows greatly improved performance over PEDOT:PSS ink, greatly reducing power consumption.

Liu et al. produced inkjet printed force sensors using inkjet printed P(VDF-TrFE-CTFE) on top of sputtered Au electrodes on Kapton film [43]. The polymer was dissolved in triethyl phosphate at a concentration of 1 wt%, and multiple layers were printed before annealing at 110 °C in a vacuum chamber overnight. During printing the substrate was heated to 90 °C to favor evaporation of the solvents in the ink. The final film produced after repeated printed layers was 10 μm.

Alternatively, PEDOT:PSS can be used as an electrode material, as shown by Sborikas et al. who inkjet printed layers of PEDOT:PSS onto pre-prepared (PVDF-TrFE) film manufactured using solvent casting [44]. The conductivity of the PEDOT:PSS was shown to be a limiting factor, contributing to dielectric losses. Nonetheless, the resultant electrodes were shown to be suitable for the poling of the (PVDF-TrFE) film.

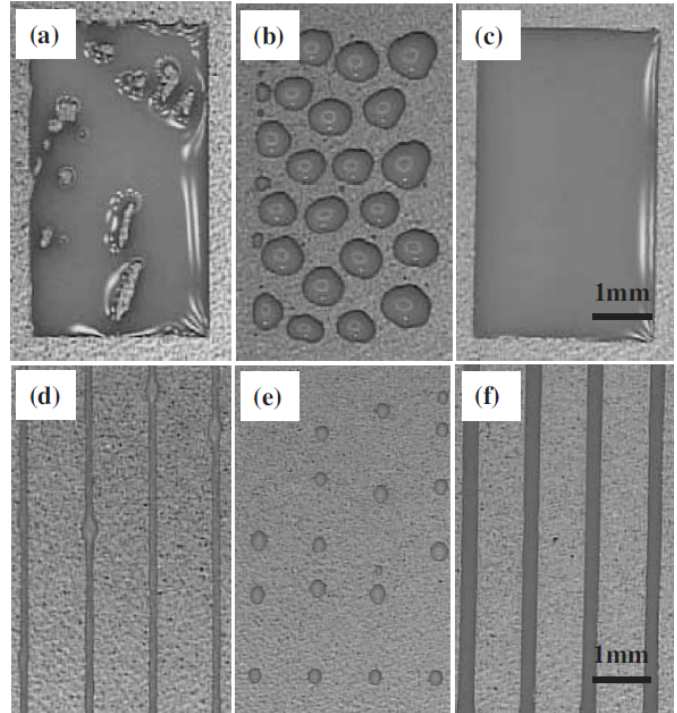


Fig. 15. Printed rectangular patterns of BaTiO<sub>3</sub> on (a) Pt electrode, (b) EC and (c) treated EC, and line patterns on (d) Pt electrode, (e) EC and (f) EC treated by inkjet printing. [46].

### B. Piezoelectric ceramic devices

Another class of piezo and ferroelectric materials commonly used are piezoelectric ceramics. Piezoelectric ceramics possess higher piezoelectric coefficients than PVDF, though suffer from brittleness and are not capable of as great deflections. Whilst most commonly produced using sputter deposition, a number of different piezoelectric ceramics actuators have also been manufactured using inkjet printing to manufacture either the electrodes, the ceramic layer, or both. Most actuators use lead zirconate titanate (PZT) for the active material. This material choice is consistent with actuators produced using conventional methods which also mostly use PZT thanks to its relative prevalence.

Ando et al. produced a PZT based bistable actuator ex-

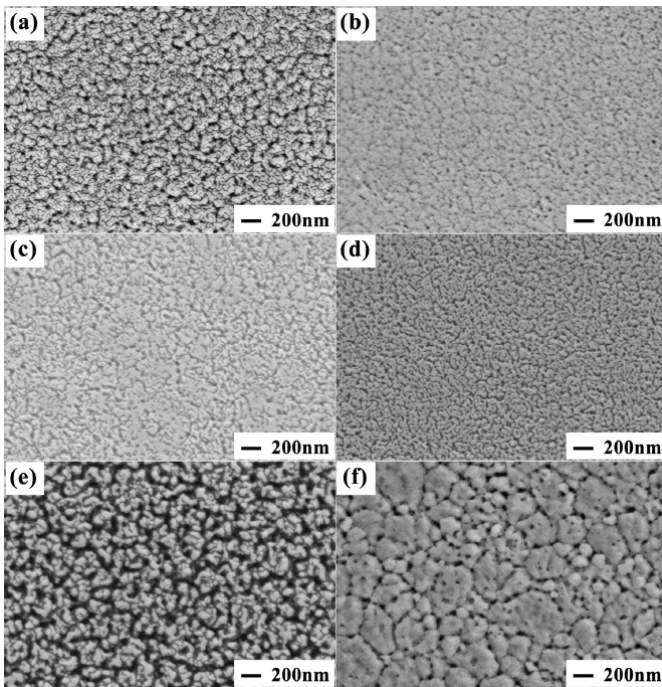


Fig. 16. Surface morphologies of inkjet printed BNT thin films annealed with: (a) 620 C wet air, (b) 650 C wet air, (c) 670 C wet air, (d) 700 C wet air, (e) 650 C dry air, (f) 670 C dry air [47].

hibiting snap through buckling using inkjet printed interdigital transducer electrodes (Fig. 14) [45]. the electrodes are printed with a commercial inkjet printer using a silver nanoparticle solution and deposited onto PET film. The PZT layer is then deposited on top of the electrodes using screen printing. In this application only the electrodes are inkjet printed, but show a compatibility for use with piezoelectric ceramics.

Kuscer et al. attempted the printing of PZT thick films, using PZT powder suspended in a dispersion of water and glycerol [48]. The ink was printed onto an aluminium oxide substrate with screen printed platinum paste electrodes. After printing, the piezoelectric layer requires sintering at 1100 °C for 1 hr in a lead oxide rich atmosphere. The produced PZT layer showed some inconsistencies in uniformity, likely due to the printing conditions. The defects present in the film prevented the actuator from being characterized. The complex preparation steps for the ink, the high sintering temperature, and the presence of several defects suggest this method requires further work before being useful.

Ferri et al. formulated a PZT based piezoelectric ink that could be deposited using inkjet printing and cured at 150 °C, a much lower temperature than the 900 °C or above typically required [49]. The ink consisted of a PZT milled powder in conjunction with a low temperature polymeric vehicle binder. This produces a screen printable ink. In order to achieve a viscosity low enough for inkjet printing, the ink is further dispersed in ethylene glycol diacetate. Once printed, the dispersion shows homogenous PZT powder content.

Yuichi et al. demonstrated the inkjet printing of BaTiO<sub>3</sub>

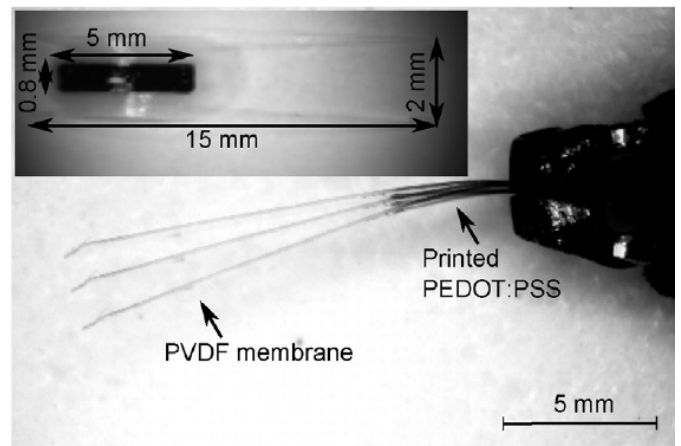


Fig. 17. Inkjet printed PEDOT:PSS actuators on PVDF membranes [51].

using a mix of BaTiO<sub>3</sub> powder in water, polyethylene glycol, polycarboxyl ammonium-based dispersant, and methyl alcohol [46]. The ink was printed on an oxygen plasma modified ethyl cellulose layer, which was spin coated on top of platinum paste electrodes screen printed on a ZrO<sub>2</sub> substrate. The BaTiO<sub>3</sub> is then dried at 130 °C, annealed at 600 °C and finally fired at 1340 °C. Treating the ethyl cellulose layer with oxygen plasma was shown to produce hydrophobicity and improve wettability of the surface. This in turn produced better inkjet printed layers with good definition of the printed patterns as shown in Fig. 15.

Soichiro et al. employed a sol-gel method for producing PZT thin films with various Zr/Ti ratios [50]. In this method, a commercial inkjet printer was used to deposit precursor solutions onto silicon wafers. The deposited solutions are then dried at 110 °C, calcinated at 350 °C, and sintered at 650 °C. It was found that inkjet printing was able to adequately mix the precursor solutions, through the deposited dots suffered from very uneven thickness.

Zhi et al. [47] utilized a similar sol-gel method to manufacture Na<sub>0.5</sub>Bi<sub>0.5</sub>TiO<sub>3</sub> (BNT) thin film from precursor solutions. A commercial inkjet printer was used to print the precursor inks onto a fluorine-doped tin oxide (FTO) glass substrate. After printing, the films were dried at 200 °C, before being heat treated at 450 °C. The final printed film is annealed at 620-700 °C in either dry or wet air (Fig. 16). It was observed that annealing the film at 670 °C in wet air produced optimal ferroelectric and dielectric properties. The final films produced using inkjet printing showered a dense and crack free microstructure.

### C. Other inkjet printed devices

A number of other inkjet printed ionic EAP actuators are also present, based on PEDOT:PSS. In these actuators, the PEDOT:PSS electrodes are printed onto an ion reservoir such as PVDF, and the ion transport during redox reactions causes the PEDOT:PSS to shrink or expand. Whilst spin coated PEDOT:PSS has significant difficulty adhering to hydrophic

PVDF, inkjet printing can deposit PEDOT:PSS with improved results [51]. Simate et al. produced conducting polymer based actuators by inkjet printing PEDOT:PSS electrodes onto a functionalised PVDF membrane, before impregnating with ionic liquid. The produced actuators achieved up to 0.45% strain at 1.5 V as shown in Fig. 17 [51].

Poldsalu et al. produced similar actuators using PEDOT:PSS and nanoporous activated carbon aerogel (ACA) printed on a commercial PVDF membrane [52]. A maximum of 0.7% ACA could be added to the PEDOT:PSS ink solution. The strain achieved at 1 V was 0.1% and 0.2% for PEDOT:PSS-ACA and pure PEDOT:PSS electrodes respectively. The addition of ACA increased the stress, and it was shown PEDOT:PSS-ACA was suitable for actuators desiring a high force whilst PEDOT:PSS was suitable for actuators desiring high strain.

Poldsalu et al. also produced actuators consisting of PEDOT:PSS electrodes inkjet printed on a interpenetrating polymer network (IPN) thin film composed of nitrile butadiene rubber and poly(ethylene oxide) [53]. The actuators were tested in aqueous and organic (propylene carbonate) solutions of bis(trifluoromethane)sulfonimide lithium salt (LiTFSI) as electrolytes, and in air whilst using an ionic liquid. When excited by a 0.65 to -0.6 V square wave, the actuators achieved 3% strain in aqueous electrolyte, 1% in propylene carbonate, and 0.14% in the ionic liquid.

## VII. DISCUSSION AND CONCLUSION

The printing of conductive nanoparticle inks is well established and can be done using a commercial inkjet printer. The most commonly used silver nanoparticle inks require thermal or photonic post processing and may not be suitable for use in combination with low melting temperature polymers. Chemically sintering silver inks have lackluster performance when not printed on the specific substrates they are suited for. Although more affordable than silver, copper inks require photonic sintering and can only be sintered by certain wavelengths. Whilst carbon black nanoparticle inks have lower conductivity than both silver and copper inks, they only require drying and do not contribute to the effective stiffness of an actuator in the way a sintered silver film does.

A number of fully inkjet printed P(VDF-TrFE) actuators exist, all using silver ink for the electrode material. P(VDF-TrFE-CTFE) has also been successfully inkjet printed, though on sputtered Au electrodes. The printing of polymers represents a significant challenge that has been achieved with industrial inkjet printers, but not yet with a commercial inkjet printer. Compared to P(VDF-TrFE), the terpolymer P(VDF-TrFE-CTFE) offers improved electromechanical strains and extremely high electrostriction. As of this point there are no P(VDF-TrFE-CTFE) based actuators with inkjet printed electrodes.

The printing of piezoelectric ceramic actuators has not been fully realized, with mostly only ceramic layers being printed rather than full actuators. Most printed piezoelectric ceramics require complex preparation of precursor solutions or very high temperature sintering steps. The overall manufacture is

very complex and time consuming, requiring a significant amount of equipment and material in addition to an inkjet printer.

The printing of PEDOT:PSS actuators involve the printing of polymer electrodes, which present a significantly greater challenge than the printing of conductive ink electrodes for the reasons described in Section V. All inkjet printed PEDOT:PSS actuators used industrial grade printers to print the polymer layer and have complex manufacturing steps not easily achievable with commercial inkjet printers. In addition to this, they also require a form of ionic fluid to function and cannot achieve the same bandwidth as P(VDF-TrFE-CTFE) actuators.

Based on these reasons it was decided to focus on the development of inkjet printed carbon black electrode P(VDF-TrFE-CTFE) actuators, manufactured using a commercial inkjet printer. This would be the first ferroelectric polymer actuator manufactured using inkjet printed carbon black electrodes, and would prove the viability of carbon black as an electrode material in this application. Using a commercial inkjet printer to print the electrodes would allow the manufacturing process to be simplified as well as economized significantly. The polymer choice of P(VDF-TrFE-CTFE) would produce an actuator with greater deflections and electromechanical strains than previously achieved in literature by partly or fully inkjet printed P(VDF-TrFE) actuators.

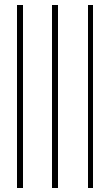
## REFERENCES

- [1] S. T. Kwang J. Kim, *Electroactive Polymers for Robotic Applications*. Springer-Verlag London, 2007, vol. 23.
- [2] Y. Bar-Cohen, *Electroactive Polymers as Artificial Muscles - Reality and Challenges*, 2001.
- [3] A. Hunt, "Application-oriented performance characterization of the ionic polymer transducers (ipts)," Thesis, 2017.
- [4] G. Shuxiang, T. Fukuda, K. Kosuge, F. Arai, K. Oguro, and M. Negoro, "Micro catheter system with active guide wire," in *Proceedings of 1995 IEEE International Conference on Robotics and Automation*, vol. 1, Conference Proceedings, pp. 79–84 vol.1.
- [5] 1998, "Ferroelectricity". [Online]. Available: <https://www.britannica.com/science/ferroelectricity>
- [6] K. C. Kao, *Dielectric Phenomena in Solids*, 2004.
- [7] H. Ohigashi, K. Koga, M. Suzuki, T. Nakanishi, K. Kimura, and N. Hashimoto, "Piezoelectric and ferroelectric properties of p(vdf-trfe) copolymers and their application to ultrasonic transducers," *Ferroelectrics*, vol. 60, no. 1, pp. 263–276, 1984.
- [8] H. Xu, Z. Y. Cheng, D. Olson, T. Mai, Q. M. Zhang, and G. Kavarnos, "Ferroelectric and electromechanical properties of poly(vinylidene-fluoridetrifluoroethylenechlorotrifluoroethylene) terpolymer," *Applied Physics Letters*, vol. 78, no. 16, pp. 2360–2362, 2001. [Online]. Available: <https://doi.org/10.1063/1.1358847>
- [9] R. Perez, M. Krl, and H. Bleuler, "Study of polyvinylidene fluoride (pvdf) based bimorph actuators for laser

- scanning actuation at khz frequency range,” *Sensors and Actuators A: Physical*, vol. 183, pp. 84–94, 2012.
- [10] L. Engel, K. R. V. Volkinburg, M. Ben-David, G. N. Washington, S. Krylov, and Y. Shacham-Diamand, “Fabrication of a self-sensing electroactive polymer bimorph actuator based on polyvinylidene fluoride and its electrostrictive terpolymer,” in *SPIE Smart Structures and Materials + Nondestructive Evaluation and Health Monitoring*, vol. 9798. SPIE, Conference Proceedings, p. 11.
- [11] B. Ando, S. Baglio, A. R. Bulsara, T. Emery, V. Marletta, and A. Pistorio, “Low-cost inkjet printing technology for the rapid prototyping of transducers,” *Sensors (Basel)*, vol. 17, no. 4, 2017.
- [12] H. Rubaiyet Iftekarul, V. Rmy, G. Michel, V. Laurie, B. Patrick, and B. Xavier, “Inkjet printing of high molecular weight pvdf-trfe for flexible electronics,” *Flexible and Printed Electronics*, vol. 1, no. 1, p. 015001, 2016.
- [13] J. Perelaer and U. S. Schubert, *8.07 - Ink-Jet Printing of Functional Polymers for Advanced Applications*. Amsterdam: Elsevier, 2012, pp. 147–175.
- [14] K. K. B. Hon, L. Li, and I. M. Hutchings, “Direct writing technology advances and developments,” *CIRP Annals*, vol. 57, no. 2, pp. 601–620, 2008.
- [15] Y. Kawahara, S. Hodges, B. S. Cook, C. Zhang, and G. D. Abowd, “Instant inkjet circuits: lab-based inkjet printing to support rapid prototyping of ubicomp devices,” in *Proceedings of the 2013 ACM international joint conference on Pervasive and ubiquitous computing*. 2493486: ACM, Conference Proceedings, pp. 363–372.
- [16] G.-K. Lau and M. Shrestha, “Ink-jet printing of micro-electro-mechanical systems (mems),” *Micromachines*, vol. 8, no. 6, 2017.
- [17] “Novacentrix Conductive Inks Summary”. [Online]. Available: [https://www.novacentrix.com/sites/default/files/pdf/NovaCentrix\\_Inks\\_Summary\\_web.pdf](https://www.novacentrix.com/sites/default/files/pdf/NovaCentrix_Inks_Summary_web.pdf)
- [18] 2016, “Data Sheet: MetalonJS-B25P”. [Online]. Available: [https://www.novacentrix.com/sites/default/files/pdf/Metalon%20JS-B25P\\_1.pdf](https://www.novacentrix.com/sites/default/files/pdf/Metalon%20JS-B25P_1.pdf)
- [19] 2018, “Data Sheet: MetalonJS-A102A”. [Online]. Available: <https://www.novacentrix.com/sites/default/files/pdf/Metalon%20JS-A102A%20rev1.pdf>
- [20] E. S. Park, Y. Chen, T.-J. K. Liu, and V. Subramanian, “A new switching device for printed electronics: Inkjet-printed microelectromechanical relay,” *Nano Letters*, vol. 13, no. 11, pp. 5355–5360, 2013.
- [21] O. Pabst, J. Perelaer, E. Beckert, U. S. Schubert, R. Eberhardt, and A. Tnnermann, “All inkjet-printed piezoelectric polymer actuators: Characterization and applications for micropumps in lab-on-a-chip systems,” *Organic Electronics*, vol. 14, no. 12, pp. 3423–3429, 2013.
- [22] “Genesink Smartink Product Overview”. [Online]. Available: <https://www.genesink.com/smartink/>
- [23] 2012, “Photonic Sintering of Silver for Roll-to-Roll Printed Electronics”. [Online]. Available: [http://www.xenoncorp.com/files/4114/3767/5822/Photonic\\_Sintering\\_of\\_Silver\\_for\\_Roll-to-Roll\\_Printed\\_Electronics\\_-\\_2012.pdf](http://www.xenoncorp.com/files/4114/3767/5822/Photonic_Sintering_of_Silver_for_Roll-to-Roll_Printed_Electronics_-_2012.pdf)
- [24] K. A. Schroder, *Mechanisms of photonic curing: Processing high temperature films on low temperature substrates*, 2011, vol. 2.
- [25] 2009. [Online]. Available: <http://www.freepatentsonline.com/y2009/0233237.html>
- [26] J. Kastner, T. Faury, H. M. Auerhuber, T. Obermiller, H. Leichtfried, M. J. Haslinger, E. Liftingner, J. Innerlohinger, I. Gnatiuk, D. Holzinger, and T. Lederer, “Silver-based reactive ink for inkjet-printing of conductive lines on textiles,” *Microelectronic Engineering*, vol. 176, pp. 84–88, 2017.
- [27] A. Soltani, B. K. Vahed, A. Mardoukhi, and M. Mntysalo, “Laser sintering of copper nanoparticles on top of silicon substrates,” *Nanotechnology*, vol. 27, no. 3, p. 035203, 2016.
- [28] B. K. Park, D. Kim, S. Jeong, J. Moon, and J. S. Kim, “Direct writing of copper conductive patterns by ink-jet printing,” *Thin Solid Films*, vol. 515, no. 19, pp. 7706–7711, 2007.
- [29] S. Lim, M. Joyce, P. Fleming, A. Aijazi, and M. Atashbar, *Inkjet Printing and Sintering of Nano-Copper Ink*, 2013, vol. 57.
- [30] J. Niittynen, E. Sowade, H. Kang, R. R. Baumann, and M. Mntysalo, “Comparison of laser and intense pulsed light sintering (ipl) for inkjet-printed copper nanoparticle layers,” *Scientific Reports*, vol. 5, p. 8832, 2015.
- [31] 2017, “Data Sheet: CI-004”. [Online]. Available: [http://intrinsiqmaterials.com/wp-content/uploads/2018/04/CI-004\\_Data\\_Sheet\\_2017\\_v1.3.pdf](http://intrinsiqmaterials.com/wp-content/uploads/2018/04/CI-004_Data_Sheet_2017_v1.3.pdf)
- [32] C. A. d. Saint-Aubin, S. Rosset, S. Schlatter, and H. Shea, “High-cycle electromechanical aging of dielectric elastomer actuators with carbon-based electrodes,” *Smart Materials and Structures*, vol. 27, no. 7, p. 074002, 2018.
- [33] S. Schlatter, S. Rosset, and H. Shea, “Inkjet printing of carbon black electrodes for dielectric elastomer actuators,” in *SPIE Smart Structures and Materials + Nondestructive Evaluation and Health Monitoring*, vol. 10163. SPIE, Conference Proceedings, p. 9.
- [34] P. Beecher, P. Servati, A. Rozhin, A. Colli, V. Scardaci, S. Pisana, T. Hasan, A. J. Flewitt, J. Robertson, G. W. Hsieh, F. M. Li, A. Nathan, A. C. Ferrari, and W. I. Milne, “Ink-jet printing of carbon nanotube thin film transistors,” *Journal of Applied Physics*, vol. 102, no. 4, p. 043710, 2007.
- [35] T. Kim, H. Song, J. Ha, S. Kim, D. Kim, S. Chung, J. Lee, and Y. Hong, “Inkjet-printed stretchable single-walled carbon nanotube electrodes with excellent mechanical properties,” *Applied Physics Letters*, vol. 104, no. 11, p. 113103, 2014.
- [36] T. Wang, M. A. Roberts, I. A. Kinloch, and B. Derby, “Inkjet printed carbon nanotube networks: the influence of drop spacing and drying on electrical properties,” *Journal of Physics D: Applied Physics*, vol. 45, no. 31, p. 315304, 2012.

- [37] B. Curdin, G. Samuele, A. Hatem, and K. Gabor, "Inkjet printed multiwall carbon nanotube electrodes for dielectric elastomer actuators," *Smart Materials and Structures*, vol. 25, no. 5, p. 055009, 2016.
- [38] K.-Y. Shin, J.-Y. Hong, and J. Jang, "Flexible and transparent graphene films as acoustic actuator electrodes using inkjet printing," *Chemical Communications*, vol. 47, no. 30, pp. 8527–8529, 2011.
- [39] Z. Du, X. Yu, and Y. Han, "Inkjet printing of viscoelastic polymer inks," *Chinese Chemical Letters*, vol. 29, no. 3, pp. 399–404, 2018.
- [40] S. Zhang, B. Neese, K. Ren, B. Chu, F. Xia, T. Xu, S. Tadigadapa, Q. Wang, Q. M. Zhang, and F. Bauer, "Relaxor ferroelectric polymers, thin film devices, and ink-jet microprinting for thin film device fabrication," *Ferroelectrics*, vol. 342, no. 1, pp. 43–56, 2006.
- [41] D. Soltman and V. Subramanian, "Inkjet-printed line morphologies and temperature control of the coffee ring effect," *Langmuir*, vol. 24, no. 5, pp. 2224–2231, 2008.
- [42] D. Thuau, K. Kallitsis, F. D. Dos Santos, and G. Hadziioannou, "All inkjet-printed piezoelectric electronic devices: energy generators, sensors and actuators," *Journal of Materials Chemistry C*, vol. 5, no. 38, pp. 9963–9966, 2017.
- [43] Q. Liu, "Development of electrostrictive p(vdf-trfe-ctfe) terpolymer for inkjet printed electromechanical devices," Thesis, 2016.
- [44] M. Sborikas, B. Fischer, and M. Wegener, "Piezo- and ferroelectric p(vdf-trfe) films with inkjet-printed pedot:pss electrodes: Preparation parameters and property evaluation," in *2014 Joint IEEE International Symposium on the Applications of Ferroelectric, International Workshop on Acoustic Transduction Materials and Devices & Workshop on Piezoresponse Force Microscopy*, Conference Proceedings, pp. 1–4.
- [45] B. And, S. Baglio, A. R. Bulsara, V. Marletta, V. Ferrari, and M. Ferrari, "A low-cost snap-through-buckling inkjet-printed device for vibrational energy harvesting," *IEEE Sensors Journal*, vol. 15, no. 6, pp. 3209–3220, 2015.
- [46] S. Yuichi, F. Tomoaki, and A. Masatoshi, "Preparation of batio 3 thick films by inkjet printing on oxygen-plasma-modified substrates," *Japanese Journal of Applied Physics*, vol. 45, no. 9S, p. 7247, 2006.
- [47] Z. Cheng and Z. Zhao, "Ink-jet printed bnt thin films with improved ferroelectric properties via annealing in wet air," *Ceramics International*, vol. 44, no. 9, pp. 10700–10707, 2018.
- [48] D. Kuscer, O. Noshchenko, H. Uri, and B. Mali, "Piezoelectric properties of ink-jetprinted lead zirconate titanate thick films confirmed by piezoresponse force microscopy," *Journal of the American Ceramic Society*, vol. 96, no. 9, pp. 2714–2717, 2013.
- [49] M. Ferrari, V. Ferrari, M. Guizzetti, and D. Marioli, "Piezoelectric low-curing-temperature ink for sensors and power harvesting," in *Sensors and Microsystems*, P. Malcovati, A. Baschiroto, A. d'Amico, and C. Natale, Eds. Springer Netherlands, Conference Proceedings, pp. 77–81.
- [50] O. Soichiro, T. Rie, and S. Tadashi, "Fabrication of ferroelectric pb(zr,ti)o 3 thin films with various zr/ti ratios by ink-jet printing," *Japanese Journal of Applied Physics*, vol. 41, no. 11S, p. 6714, 2002.
- [51] A. Simate, F. Mesnilgrete, B. Tondu, P. Soures, and C. Bergaud, "Towards inkjet printable conducting polymer artificial muscles," *Sensors and Actuators B: Chemical*, vol. 229, pp. 425–433, 2016.
- [52] I. Poldsalu, M. Harjo, T. Tamm, M. Uibu, A.-L. Peikolainen, and R. Kiefer, "Inkjetprinted hybrid conducting polymer-activated carbon aerogel linear actuators driven in an organic electrolyte," *Sensors and Actuators B: Chemical*, vol. 250, pp. 44–51, 2017.
- [53] I. Poldsalu, K. Rohtlaid, T. M. G. Nguyen, C. Plesse, F. Vidal, M. S. Khorram, A.-L. Peikolainen, T. Tamm, and R. Kiefer, "Thin ink-jet printed trilayer actuators composed of pedot:pss on interpenetrating polymer networks," *Sensors and Actuators B: Chemical*, vol. 258, pp. 1072–1079, 2018.





# P(VDF-TrFE-CTFE) Actuators with Inkjet Printed Electrodes

This paper details the manufacturing of a P(VDF-TrFE-CTFE) ferroelectric polymer actuator with inkjet printed carbon black electrodes. A 3×18 mm cantilever actuator is produced, and characterized in both static and dynamic actuation. My contributions for this conference paper include the manufacturing process, characterization, data processing, and leading of the report writing. This paper was submitted the ICCMA 2019 conference.



# P(VDF-TrFE-CTFE) Actuators with Inkjet Printed Electrodes

K. Keith Baelz and \*Andres Hunt

*Department of Precision and Microsystems Engineering*

*Faculty Mechanical, Maritime and Materials Engineering (3mE), Delft University of Technology*

Mekelweg 2, 2628 CD Delft, The Netherlands

Email: \*A.Hunt-1@tudelft.nl, Phone: \*+31 6 4005 0774

**Abstract**—Piezoelectric inkjet printing has proven its potential for use as an additive manufacturing technique for depositing thin films, and can be especially useful in the rapid prototyping of devices such as PCBs, energy harvesters, capacitive sensors, or RFID antennae. The increasing availability of conductive inkjet inks of various compositions offer the means to print conductive patterns with relative ease in very little time. Whilst conductive inks are typically used to print conductive circuitry, the possibility of printing more modern and better performing smart materials opens the path for fully inkjet printed active devices. This offers the potential to manufacture smart materials and actuators faster, more economically, and with better repeatability than when using masking or photolithographic processes, without requiring specialized machinery or facilities. In this paper, we employ a low cost approach to manufacture 4 layer relaxor ferroelectric cantilever actuators using a commercial inkjet printer. A carbon black nanoparticle dispersion is printed onto an absorbent substrate to form a conductive bottom electrode, before a layer of P(VDF-TrFE-CTFE) is applied on top as the active material. Finally an additional layer of carbon black is printed on top of the polymer to form the top electrode. The finished actuators are poled to induce piezoelectric behavior in addition to the existing electrostrictive behavior. The resultant actuators can achieve deflections of up to 207  $\mu\text{m}$  under loads of 300 V, and can achieve over 3mm deflection when operating at resonance frequencies of 110-130 Hz.

## I. INTRODUCTION

Printable smart materials have the potential to significantly simplify and economize the manufacture of complex active devices in both rapid prototyping for research as well as industrial processes such as roll to roll processing [1]. The manufacture of PVDF based electroactive polymer actuators has been traditionally achieved using microelectronic photolithography methods. This represents a complex multi-step process requiring specialized equipment whilst imposing limitations on the size of the manufactured devices. Developments in the field of inkjet manufacturing in conjunction with the rising prevalence in use of P(VDF-TrFE-CTFE) as an active material open the possibility to produce actuators exhibiting significantly improved strains with a level of flexibility and simplicity of manufacture not traditionally possible.

As an additive manufacturing method, inkjet printing requires less machinery, reduces raw material cost thanks to reduced waste, and provides the benefits of being able to produce new designs without the need to prepare masks or stencils [3]. Inkjet printing has garnered significant interest as a contact free additive manufacturing method capable of producing thin films with great versatility. Inkjet printing has

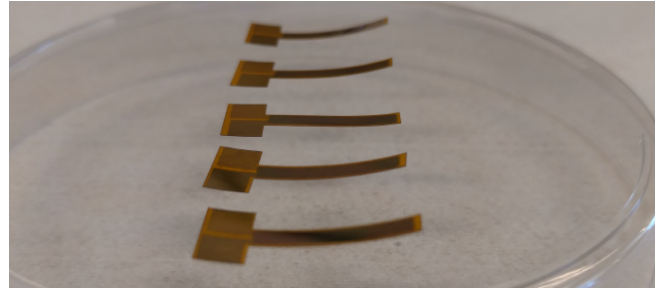


Fig. 1. Samples of P(VDF-TrFE-CTFE) actuators produced in TU Delft with sputter coated electrodes [2].

previously demonstrated its viability as a method to produce wiring and PCB prototypes through the use of conductive nanoparticle inks [4]. Such inks are available in a wide variety of compositions and materials, commonly consisting of metal nanoparticle dispersions.

Carbon black nanoparticle inks have been shown to function as a suitable electrode material used with silicone based dielectric elastomer actuators [5], and require no thermally intensive post processing to function. This is in contrast to metal nanoparticle based inks which typically require elevated temperatures to sinter and achieve conductivity, and as such are rarely suitable for use with temperature sensitive polymer substrates. In addition to printing conductive inks, the possibility of printing electroactive polymers has enabled a class of fully inkjet printed sensors and actuators [6, 7, 8, 9]. Such devices most typically use P(VDF-TrFE) as the active material in conjunction with silver electrodes [6, 7]. The polymers are prepared for printing by dissolving them in a volatile solvent such as MEK or cyclopentanone in addition to a solvent with a high boiling point such as DMSO to prevent evaporation and clogging in the printer nozzles [10]. The printing of polymer materials represents a significant challenge due to the non-Newtonian properties of polymer ink in addition to high viscosity [11]. It is rarely possible to use over 1%wt. of polymer in inks and still achieve consistent and even jetting [6, 10].

In this paper we report a methodology for the manufacture of P(VDF-TrFE-CTFE) that allows simpler manufacturing whilst maintaining comparable performance to similar actuators previously produced at TU Delft [2], shown in Fig. 1. The electrodes are applied by printing repeated layers of

carbon black nanoparticle ink, and the electroactive polymer is applied in multiple spin coated layers. The performance of both poled and unpoled samples, and samples with different polymer layer counts are investigated.

## II. MATERIALS AND METHODS

### A. Printer selection and actuator materials

Printing the electrodes requires a flat printing bed with decent precision, capable of jetting ink on the same regions repeatedly consistently across several printing cycles. The substrate being printed on should remain as still as possible with minimal flexing or bending as to avoid damaging or altering the printed layer in undesired ways. The printer must also not smudge ink that remains wet after initial deposition. Based on these requirements, a commercial printer with a CD printing tray would function as a suitable printing bed on which substrate could be mounted. In order to be able to print custom conductive inks and refill the cartridges, the printer model chosen must also have compatible chip resetters or resettable refillable cartridges. Based on the requirement of CD printing capabilities and availability of refillable cartridges, the printer selected for the manufacturing was the Epson Expression Premium XP 900.

As the electrodes and active polymer on their own do not possess the required structural stiffness to be useful as an actuator, they therefore have to be deposited on a substrate. The substrate chosen  $140 \pm 12 \mu\text{m}$  PET film coated in a micro-porous resin (Novele IJ-220, Novacentrix) [12]. This substrate is specifically designed for use with inkjet printed conductive nanoparticle inks and produced more even ink distribution and consistent film thickness compared to nonabsorbent substrates such as untreated PEN or Kapton. Conductive inks printed on Novele substrate were found to dry and become conductive near instantaneously with perfect repeatability whereas inks printed on Kapton or PEN would require post processing and would rarely deposit in even thickness over larger regions. Conductive inks printed on Novele also produced consistently better conductivity than on any other substrate. Novele however begins to curl past  $100^\circ\text{C}$ , and as such is not suitable for use with inks that require treating at temperatures significantly above  $100^\circ\text{C}$ .

The conductive ink selected was a carbon black nanoparticle dispersion in ethylene glycol with 3.5% solid material loading specially formulated for use with consumer printers (JR-700LV, Novacentrix) [13]. The advantage of carbon black inks over more conventionally used silver inks is that they do not require any form of sintering or post processing beyond drying. Thermal sintering would run the risk of damaging the substrate or ferroelectric polymer, whilst photonic sintering would require special machinery. Thus the elimination of sintering altogether presents a significant advantage.

The ferroelectric polymer chosen is a P(VDF-TrFE-CTFE) powder (PVDF:TrFE:CTFE = 62:31:7 in mol%) (PIEZOTECH ARKEMA) [14]. This relaxor ferroelectric polymer exhibits high electrostrictive strain with above 5% electromechanical deformation possible [14]. The electromechanical properties

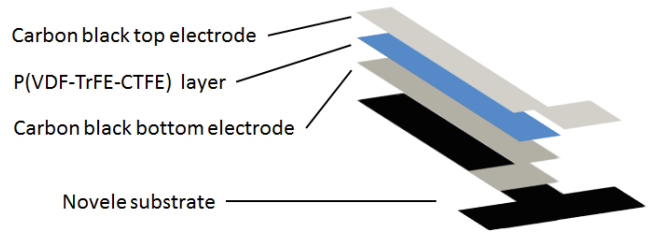


Fig. 2. Layered structure of the actuator.

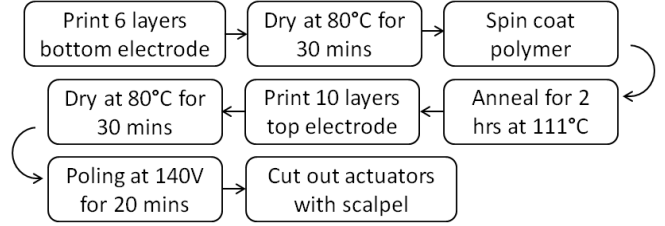


Fig. 3. Manufacturing steps for ferroelectric polymer actuators with inkjet printed carbon black electrodes.

of this polymer along with its high breakdown voltage make it particularly well suited for use in flexible actuators.

### B. Manufacturing

In this paper, we manufactured actuators based on a 4 layer structure in which all layers are applied on top of each other sequentially as shown in Fig. 2. The layers from bottom to top are the PET substrate, the printed bottom electrode, the spin coated ferroelectric polymer, and the printed top electrode. The electrodes are routed to two contact pads at the base where a voltage supply can be connected. The ferroelectric polymer is only applied to the cantilever region and not to the base, to allow a conductive contact point with the bottom electrode. The process is outlined in Fig. 3.

1) *Bottom electrode:* To manufacture the actuator, the first step is to print the bottom electrode. As the CD printing function is being used for manufacture, it is necessary to use the Epson Print CD software suitable for the printer. This is the easiest way to print a desired pattern onto the CD region without the need for any prior alteration in hardware or software. The pattern desired to be printed is generated as a PNG file and positioned onto a CD in the software. To deposit as much ink as possible, the medium is set to "CD/DVD Premium Surface" and the printing color correction is set to the darkest option. To achieve proper coverage, it was observed that after 6 printed layers the printed region becomes fully opaque and shows no voids or defects. A strip of Novele substrate is mounted to the surface on the CD in the location of the area to be printed on. Once all layers are printed, the bottom electrode is dried at  $80^\circ\text{C}$  for 30 minutes to ensure complete solvent evaporation. Although the substrate rapidly wicks away the solvent in the ink and leaves behind only the solid carbon black material without any thermal treatment, this step is taken to ensure the ink is

completely dry. The temperatures required to sinter and render silver ink conductive would far exceed the melting point of the ferroelectric polymer and would damage the substrate. The use of carbon black inks reduced the time required for manufacture by eliminating complex post processing steps, and lowered the material cost thanks to their relative affordability compared to silver inks. Given that the carbon black only requires heating, it also eliminated the need for any specialist post processing machinery such as photonic curing tools.

2) *Polymer layer:* The next step of manufacture is the application the ferroelectric polymer. Due to complications in printing the polymer using a commercial printer, it was decided to instead use spin coating. As preparation for spin coating the P(VDF-TrFE-CTFE) powder is mixed with 2-Butanone (MEK) at a ratio of 1:10, and left in a dessicator to eliminate bubbles that were introduced during agitation. The polymer is then spin coated (SPIN150i/200i, Polos) on top of the printed bottom electrode at 1500 rpm with an acceleration of 150 rpm/s for 30 s.

The prepared polymer solvent mixture is poured over the full region desired to be coated with polymer and left to rest for 30s. This allows all the bubbles in the substrate to rise up and escape the polymer before spin coating, minimizing the number of defects in the final spin coated polymer layer. Due to the porosity of the substrate, there is air trapped inside the substrate and underneath the printed electrodes. When depositing the polymer solvent mixture onto the printed bottom electrode for spin coating, the mixture is pulled into the highly absorbent substrate and the displaced air is expelled from the substrate upwards, forming bubbles inside the polymer. If the polymer mixture is too viscous, the air bubbles have trouble rising to the top of the dispensed polymer and escaping. Due to the porous nature of the printed carbon black electrodes, the air bubbles underneath the carbon black can easily permeate the electrode layer and travel upwards and escape.

Multiple layers of polymer are added to ensure full insulation between the top and bottom electrodes. An effect of the absorbent substrate is that the polymer is sucked into the substrate and electrode rather than forming a layer on top. If the top electrode is printed directly onto a singular spin coated polymer layer, the ink will seep through and make contact with the bottom electrode. This causes a short circuit and will cause the actuator is spark or burn at relatively low voltages. Extremely viscous polymer solutions spin coated at low speeds still encounter this issue. The first layer is allowed to dry before repeating the spin coating procedure if additional layers of polymer are to be added. Once the desired number of layers have been applied, the sample is annealed for 2 hrs at 111 °C. The minimum annealing temperature of the polymer is 110 °C, whilst the melting temperature is 122 °C. The temperature must not exceed the melting point of the polymer as per manufacturer instruction. All post processing steps consisted of purely thermal treatments below 110 °C, made possible by the use of carbon black conductive ink.

3) *Top electrode:* The third step in manufacture is the printing of the top electrode. The top electrode is printed

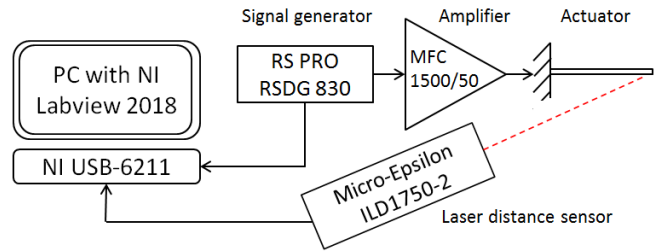


Fig. 4. Experimental setup diagram for characterizing actuators.

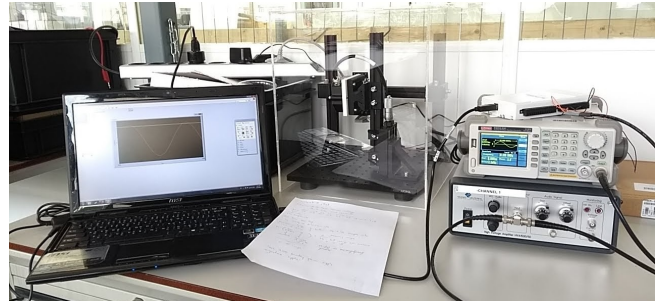


Fig. 5. Experimental setup for actuator characterization.

directly onto the dry polymer. Due to the polymer surface being nonabsorbent the ink reacts very differently from when printed on the substrate and remains wet at room temperature. The top electrode required 8-10 layers to be printed before full even coverage is achieved. This electrode is dried for 30 minutes at 80 °C to remove solvents. The surface of the wet ink will show a very noticeable orange peel effect, but will even out and become flat once dried. It is easy to tell when the top electrode is fully dry, as it will attain a matte black appearance. Any moisture left over in the ink reduces the conductivity very significantly, making this final drying step very important.

4) *Poling:* The final step in manufacture is the poling of the actuator. The actuators are connected at their contact pads to a power supply at 140 V (ES 300-0.45 DC Bench Power Supply, Delta Elektronika) and placed in a petri dish on a hot plate (UC 150, Stuart Equipment) at 85 °C. A thermocouple probe (Omega 871A Digital Thermometer, Omega Engineering) is placed on the plate next to the samples to verify temperature. Once the samples reach temperature, the power supply is turned on and the samples are allowed to pole for 20 minutes. After the 20 minutes has elapsed, the hotplate is turned off and the samples are allowed to cool whilst the power supply remains on. When the samples reach ambient temperature, the power supply can be disconnected and poling is complete. When ready for use, the actuators are cut out using a scalpel rather than laser cutting, to avoid degradation of the ferroelectric polymer due to thermal effects.

### C. Characterization set-up

In order to characterize the performance of the actuator, it is necessary to measure the deflection achieved from steady

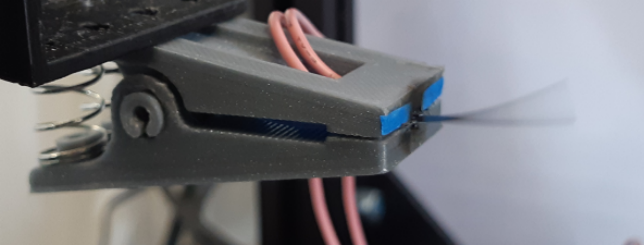


Fig. 6. Actuator clamped in characterization setup operating at resonance excited at 300V.

state voltages as well as AC voltages. The diagram of the experimental setup are shown in Fig. 4 and Fig. 5 respectively. Measurements for hysteresis and deflection with DC and AC voltage sources are taken with a setup consisting of a waveform generator (RSDG 830, RS PRO), fed into a high voltage amplifier (MFC 1500/50, Smart Materials). The amplifier amplifies the input voltage signal  $200\times$ , and is connected directly to the contact pads of the actuator via a clamp at its base. The actuator is clamped in a horizontal position for all readings taken. The resultant deflection of the actuator is measured using a laser distance sensor (ILD1750-2, Micro-Epsilon) aimed at the tip of the cantilever, which is sent into a data acquisition board (NI USB-6211, National Instruments) along with the input signal from the function generator and recorded using LabVIEW 2018. This allows the input and output signal to be recorded simultaneously and compared. The the actuator, clamp, and laser distance sensor are all contained inside a clear acrylic chamber to isolate the system from external disturbances or air flow, as well as to keep all electrical contacts isolated for safety purposes. The actuators have silver paste applied on their contact pads to improve contact with the electrodes on the clamp used to hold the units during testing. To determine the frequency response functions (FRFs) of the actuator, the same measurement setup is used. A chirp signal is produced using the NI USB-6211 and fed into the amplifier directly, bypassing the signal generator.

### III. RESULTS AND DISCUSSION

Four types of actuators were manufactured and characterized, namely actuators with 2 and 3 polymer layers, both in poled and unpoled variants. All samples were manufactured according to the methodology in section II-B, and measurements were taken using the setup described in section II-C. The completed actuators as well as the intermediate steps of manufacture are shown in Fig. 7. The actuators were manufactured in the form of cantilever beams with dimensions of  $3\times 18$  mm, where  $2.7\times 17.5$  mm is covered by the top electrode.

#### A. Manufacturing results

Actuators with 2 layers of polymer will show minor conductivity between the electrodes (sub-k $\Omega$  range), though the actuator will still function. Three spin coated layers will very significantly reduce conductivity between electrodes (M $\Omega$

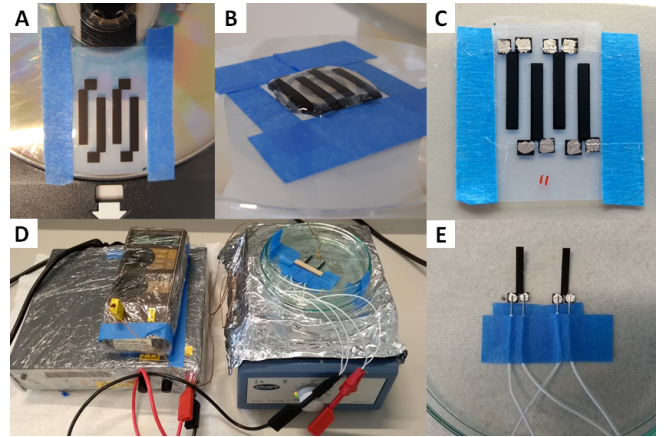


Fig. 7. Manufacturing process: A. Printing of bottom electrode, B. Spin coating of polymer layer, C. Printing of top electrode and electrode contact touch up with silver ink, D. Poling set up, E. Completed actuator units.



Fig. 8. Cross-section of actuator with 3 layers of spin coated polymer.

range). Microscopy image of an actuator with 3 spin coated layers of polymer is shown in Fig. 8.

#### B. Testing results

The maximum deflections of the unpoled samples with 2 and 3 polymer layers were  $142\ \mu\text{m}$  and  $169\ \mu\text{m}$  respectively, whilst the maximum deflections of the poled samples with 2 and 3 polymer layers were  $175\ \mu\text{m}$  and  $206\ \mu\text{m}$  respectively. These deflections were achieved at 300 V, and deflection behavior for intermediate voltages are show in Fig. 9. The samples are subsequently excited with a 300 V amplitude sine wave signal in order to excite both the piezoelectric and electrostrictive behavior as shown in Fig. 10. The piezoelectric effect manifests weakly at such a high voltage, in order to better visualize the piezoelectric behavior, the 3 polymer layer poled sample was excited at 50, 70, 90, 110, and 130 V amplitude, and the results are shown in in Fig. 11. The resonance frequency of the cantilevers was found to range from frequency from around 110-130 Hz, and the FRFs are shown in Fig. 13. The actuator at resonance is shown in Fig. 6. The hysteresis behaviors of the poled and unpoled 3 polymer layer actuators in shown in Fig. 12.

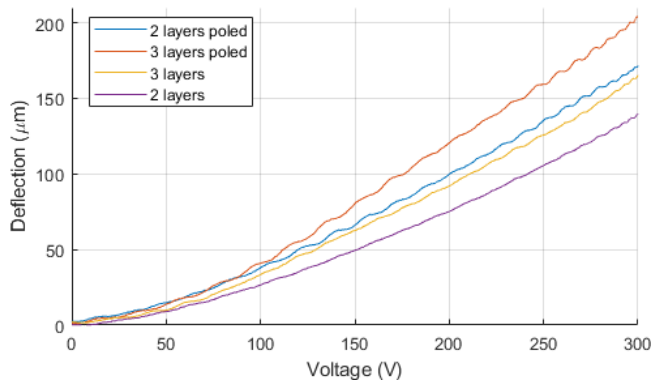


Fig. 9. Deflection of poled and unpoled actuators with increasing voltage from 0-300V.

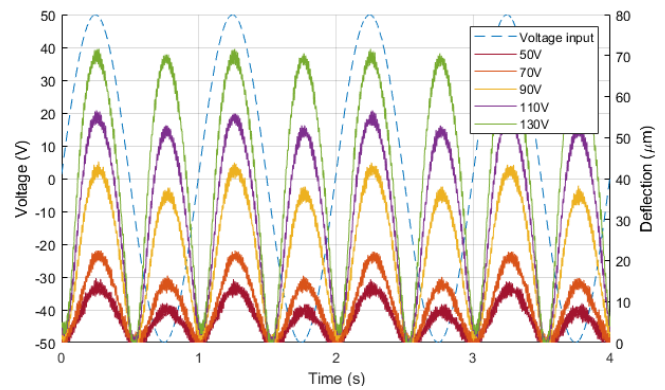


Fig. 11. Deflection of a poled 3 polymer layer actuator at different voltage amplitudes applied at 1 Hz frequency.

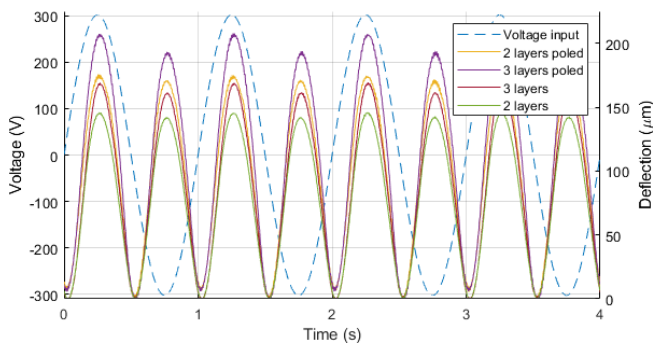


Fig. 10. Deflection of poled and unpoled actuators in response to 1 Hz sinusoidal excitation with 300 V amplitude.

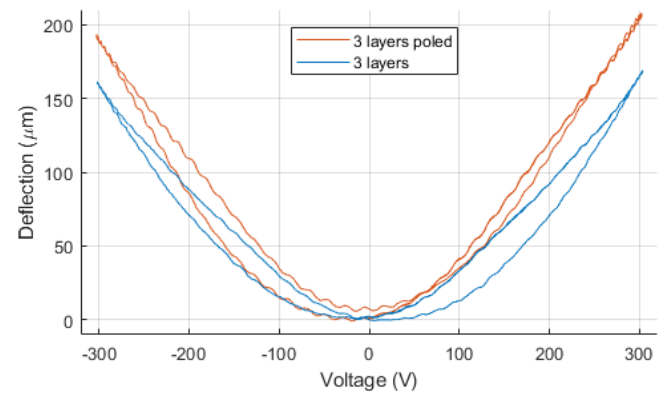


Fig. 12. Hysteresis behavior of poled and unpoled 3 polymer layer actuators.

### C. Discussion

The deflection of all samples with respect to increasing applied voltage is initially exponential, but becomes more linear at higher voltages. Excitation at voltages above 300 V are possible, but will cause some samples to fail making the data inconsistent and unreliable. The actuators with 3 layers of polymer noticeably outperform those with 2 layers, and the piezoelectric effect added by poling also shows a very clear improvement compared to the pure electrostrictive deflection shown by the unpoled samples. The 3 polymer layer actuators can also be subjected to much higher input voltages than the 2 polymer layer actuators thanks to the reduced or complete lack of conductivity between the top and bottom electrodes. Some samples with minor defects would experience minor arcing between the top and bottom electrodes, where small spots of discoloration would occur, as well as producing some smoke. Interestingly, if the arcing remained localized and did not spread causing the actuator any damage beyond this, the performance of the actuator would not degrade or be altered to any measurable degree.

The unpoled samples exhibited electrostrictive behavior, showing near identical deflection under both positive and negative voltages as shown in Fig. 10. The triple polymer coated poled samples clearly exhibit additional piezoelectric effects, evident from the difference in deflection under pos-

itive and negative voltages where the piezoelectric effect is either compounding or subtracting from the electrostrictive deflection. The direction in which the piezoelectric effect acts is determined by the direction of poling. The piezoelectric effect is less visible at higher excitation voltages especially in the 2 polymer layer sample. This is to be expected, as electrostriction is a quadratic effect, whereas piezoelectricity is a linear effect. As such at higher voltages the deflection due to the electrostrictive effect will dominate. At lower excitation voltages as shown in Fig. 11, the piezoelectric behavior is much more pronounced.

In FRFs all tested samples showed minor variances in resonance between 110-130 Hz with no clear trend in regard to the number of polymer layers or poling. The variation shown is most likely to be due to differences in how the actuator was cut out of the polymer substrate, and clamping conditions. The poled actuator shows a higher magnitude of deflection compared to the unpoled actuator (Fig. 13), which is consistent with the behavior observed in Fig. 9. The shape of the spectra of the 2 samples is otherwise similar, and consistent with what is expected from a cantilever beam type actuator. When excited at resonance at 300 V, both poled and unpoled actuators show a deflection of over 3 mm, with the poled samples observably

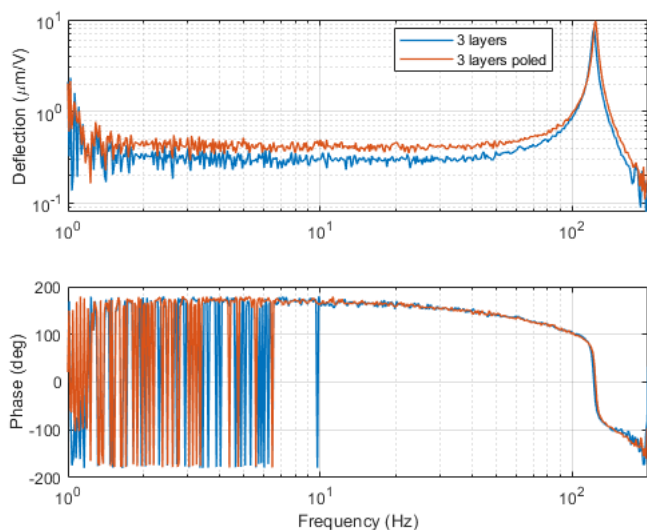


Fig. 13. Response spectra of unpoled and poled samples with 3 layers of polymer when excited with sinusoidal voltage with 50 V amplitude and 50 V offset. The deflection is due to the summation of piezoelectric and electrostrictive effects.

outperforming the unpoled samples as expected.

It was found that the behavior of all samples were consistent with conventionally manufactured P(VDF-TrFE-CTFE) actuators [2]. Compared to inkjet printed actuators produced with P(VDF-TrFE) in [7], where 145  $\mu\text{m}$  displacements were achieved at 400 V (with similar cantilever dimensions), our actuators achieved 206  $\mu\text{m}$  displacement at 300 V, representing a 42% improvement in deflection, and a 89.4% improvement in strain per volt. Whilst the actuators show significantly improved performance compared to [6] as particularly evident in FRF readings, it is not an objective comparison given the different cantilever dimensions. Therefore this paper significantly contributes to the improvement of manufacturing and performance of ferroelectric polymer actuators.

#### IV. CONCLUSIONS

In this paper we developed a methodology to produce relaxor ferroelectric polymer actuators by utilizing inkjet printed carbon black electrodes. This methodology allows the manufacture of such devices to be done much cheaper and faster than previously possible. The produced actuators were able to achieve 206  $\mu\text{m}$  steady state deflections at 300 V and 3 mm at resonance. This shows a 42% improvement in steady state deflection, and a 89.4% improvement in strain per volt compared to previously reported printed actuators of similar type, demonstrating the feasibility of the proposed manufacturing process.

#### REFERENCES

[1] B. Ando, S. Baglio, A. R. Bulsara, T. Emery, V. Marletta, and A. Pistorio, "Low-cost inkjet printing technology for

the rapid prototyping of transducers," *Sensors (Basel)*, vol. 17, no. 4, 2017.

[2] R. v. d. Nolle, "Production, design and control of p(vdf-trfe-ctfe) relaxor-ferroelectric actuators," Thesis, 2017.

[3] J. Perelaer and U. S. Schubert, *8.07 - Ink-Jet Printing of Functional Polymers for Advanced Applications*. Amsterdam: Elsevier, 2012, pp. 147–175.

[4] Y. Kawahara, S. Hodges, B. S. Cook, C. Zhang, and G. D. Abowd, "Instant inkjet circuits: lab-based inkjet printing to support rapid prototyping of ubicomp devices," in *Proceedings of the 2013 ACM international joint conference on Pervasive and ubiquitous computing*. 2493486: ACM, Conference Proceedings, pp. 363–372.

[5] S. Schlatter, S. Rosset, and H. Shea, "Inkjet printing of carbon black electrodes for dielectric elastomer actuators," in *SPIE Smart Structures and Materials + Nondestructive Evaluation and Health Monitoring*, vol. 10163. SPIE, Conference Proceedings, p. 9.

[6] D. Thuau, K. Kallitsis, F. D. Dos Santos, and G. Hadziioannou, "All inkjet-printed piezoelectric electronic devices: energy generators, sensors and actuators," *Journal of Mat. Chem. C*, vol. 5, no. 38, pp. 9963–9966, 2017.

[7] O. Pabst, J. Perelaer, E. Beckert, U. S. Schubert, R. Eberhardt, and A. Tnnermann, "All inkjet-printed piezoelectric polymer actuators: Characterization and applications for micropumps in lab-on-a-chip systems," *Organic Electronics*, vol. 14, no. 12, pp. 3423–3429, 2013.

[8] A. Simate, F. Mesnilgrete, B. Tondou, P. Soures, and C. Bergaud, "Towards inkjet printable conducting polymer artificial muscles," *Sensors and Actuators B: Chemical*, vol. 229, pp. 425–433, 2016.

[9] I. Pldsalu, K. Rohtlaid, T. M. G. Nguyen, C. Plesse, F. Vidal, M. S. Khorram, A.-L. Peikolainen, T. Tamm, and R. Kiefer, "Thin ink-jet printed trilayer actuators composed of pedot:pss on interpenetrating polymer networks," *Sensors and Actuators B: Chemical*, vol. 258, pp. 1072–1079, 2018.

[10] H. Rubaiyet Iftekharul, V. Rmy, G. Michel, V. Laurie, B. Patrick, and B. Xavier, "Inkjet printing of high molecular weight pvdf-trfe for flexible electronics," *Flexible and Printed Electronics*, vol. 1, no. 1, p. 015001, 2016.

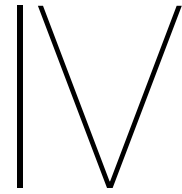
[11] Z. Du, X. Yu, and Y. Han, "Inkjet printing of viscoelastic polymer inks," *Chinese Chemical Letters*, vol. 29, no. 3, pp. 399–404, 2018.

[12] 2011, "Data Sheet: Novele IJ-220". [Online]. Available: [https://store.novacentrix.com/v/vspfiles/assets/images/novele%20ij-220\\_2212.2.pdf](https://store.novacentrix.com/v/vspfiles/assets/images/novele%20ij-220_2212.2.pdf)

[13] 2017, "Material Safety Data Sheet: JR-700LV Inkjettable Resistive Ink". [Online]. Available: <http://store.novacentrix.com/v/vspfiles/assets/images/JR-700LV%20Inkjettable%20Resistive%20Ink.pdf>

[14] 2018, "Technical Data Sheet: TDS PIEZOTECH RT-TS". [Online]. Available: <https://www.piezotech.eu/en/Technical-center/Documentation/>





# Conductivity of Inkjet Printed Nanoparticle Dispersions on Polymer Substrates

This paper details the conductive performance of silver, carbon black, and copper nanoparticle dispersions printed on PEN, Kapton, and resin coated PET substrates. Determining the conductivity of the conductive inks used for the electrodes is essential to establish what ink produces best performance in the actuators. The behavior of ink deposition across each substrate and the effect of laser photonic sintering is evaluated. The conductivity as determined through testing is used to model the cantilever actuator in the previous section, and determine the maximum achievable performance as a result of electrode resistivity.



# Conductivity of Inkjet Printed Nanoparticle Dispersions on Polymer Substrates

K. Keith Baelz

**Abstract**—Piezoelectric inkjet printing has demonstrated its potential for manufacturing conductive patterns through the use of conductive nanoparticle dispersions. In this paper we compare the performance of a number of conductive nanoparticle inks across a variety of substrates, and photonic sinter silver nanoparticles using an out-of-focus laser. The produced samples are measured to find sheet resistance to classify and compare the performance between inks. We model a ferroelectric polymer actuator to determine how the resistance of the electrode layer affects actuator performance, and through this determine what conductive inks are suitable for use in ferroelectric polymer actuator electrodes.

## I. INTRODUCTION

Inkjet printable conductive inks consist of conductive particles suspended in a fluid. Maintaining particle sizes under 50 nm in diameter help to prevent sedimentation or aggregation that would otherwise occur with larger particle sizes [14]. A higher solid material to solvent ratio will improve conductivity but raise the viscosity and increase the risk of clogging. Different piezoelectric printheads will be capable of printing different fluid viscosities, with industrial inkjet printers being capable of printing inks with much higher solid weighting than commercial inkjet printers. A number of nanoparticle materials are available, all with different conductive performance and post processing requirements. The choice of nanoparticle ink has to be matched with the printer used, the conductivity desired, and the post processing required. Certain inks will require thermal or photonic post processing that are incompatible with certain substrates, and as such the application the ink is used in will heavily dictate the choice of ink.

## II. MATERIALS AND METHODS

### A. Printer Selection and Actuator Materials

As the goal of printing conductive traces in this project is to produce electrodes for ferroelectric polymer actuators, the printing setup is the same setup as used for producing actuators in Paper 3 to maintain consistency. As such, the printer used is the Epson Expression Premium XP 900.

The substrates chosen for testing are  $125\pm 12$   $\mu\text{m}$  PEN film (Goodfellow),  $50\pm 12$   $\mu\text{m}$  Kapton film, and  $140\pm 12$   $\mu\text{m}$  PET film coated in a microporous resin (Novele IJ-220, Novacentrix) [1]. The Novele substrate is the only substrate specifically designed for use with inkjet printed conductive nanoparticle inks. Novele however begins to curl past 100 °C. In contrast, PEN film begins to shrink at 190 °C [2] and Kapton film remains stable up to 400 °C [3].

The conductive inks selected were a silver nanoparticle dispersion with 25% solid material loading (JS-B25P, Novacentrix), a carbon black nanoparticle dispersion with 3.5% solid material loading (JR-700LV, Novacentrix), a copper oxide nanoparticle dispersion with 10% solid material loading (ICI-003, Novacentrix), and a self sintering silver nanoparticle dispersion with 15% solid material loading (NBSIJ-MU01, Mitsubishi Paper Mills Ltd). All inks were specially formulated for use with consumer printers. The silver JS-B25P requires post processing in the form of either thermal sintering or photonic sintering, whilst copper ICI-003 can only be sintered photonicly. The JR-700LV carbon black and NBSIJ-MU01 silver self sintering inks do not require any post processing if printed on the Novele substrate.

### B. Manufacturing

In this paper, we print a set of test samples for each ink to compare conductivity between inks and substrates. The set consists of 10 samples of 1-10 layers printed on Novele substrate, a sample on PEN with 10 layers printed, and a sample on Kapton with 10 layers printed. All samples consist of  $15\times 20$  mm rectangles. The printing methodology is identical to the printing of the bottom electrode as shown in the Paper 3.

The 10 layer samples printed on PEN and Kapton require post processing. To dry the carbon black inks printed on Kapton and PEN film, they are placed in an oven and heated at 80 °C for 1-2 hrs until fully and evenly matte. To sinter the silver and copper inks, a laser cutter is used in lieu of a photonic sintering setup (Micro laser etching machine, Optec). In order to sinter the metal particles rather than cut through the samples, the laser is intentionally operated out of focus. For consistent results, the laser is first focused on the printed trace, and then shifted 10 mm upwards. The outline of the area to be sintered is defined in AutoCAD, and hatched with a 0.006 line spacing. The internal laser frequency is set to 10000 Hz, the diode current 3A, and constant energy if below 15000 Hz. The laser cutting parameters are described in Table I.

### C. Conductivity measurement

To measure conductivity, a 4 point probe setup is used. The 4 point probe setup consists of a probe head (SP4, Signatone) with 1.5875 mm probe spacing, a current source (2400 SourceMeter, Keithley), and a nanovoltmeter (2182 Nanovoltmeter, Keithley). The current source is set to 10  $\mu\text{A}$ , the probe tips are lowered onto center of each sample, and the voltage drop is recorded. Given that the probe spacing  $s$

TABLE I  
LASER SINTERING PARAMETERS

Speed	150
Jump Speed	200
Laser Firing Rate	50
Laser Power	50
Burst Time	1000
Repetitions	3
LaserOn Delay	0
LaserOff Delay	0
Z	0
Repetitions Objs	0
Wobble	OFF

between all probes is equal, and the film thickness  $t$  is less than half the probe spacing, the sheet resistance of the sample is given by:

$$R_s = \frac{\rho}{t} = \frac{V\pi R_1}{I \ln 2}, \quad (1)$$

where  $R_1$  is the geometric correction factor [4]. The thickness of the printed films are at most 1-2  $\mu\text{m}$  thick, meaning  $t < \frac{s}{2}$  is fulfilled. The width and height of the printed films are  $a = 20$  mm and  $b = 15$  mm respectively, therefore  $\frac{b}{s} = 9.449$  and  $\frac{a}{b} = 1.333$ . Based on this, is it possible to interpolate the geometric correction factor (K.1 Rectangular Slice) [4].  $R_1 = 0.9223$  as found using linear interpolation. The sheet resistance can therefore be simplified to:

$$R_s = 4.1802 \frac{V}{I} \quad (2)$$

#### D. Modelling the electrical behavior

A ferroelectric polymer actuator with electrodes on both sides of an insulating polymer film (as produced in Paper 3) can be approximated as an RCR ladder circuit, where the resistors are the resistance of the electrode layers, and the capacitors are the capacitance of the polymer layer in between. The greater the number of units in the ladder circuit, the better the approximation. The ladder circuit used has 5 units, and the circuit as modelled in MATLAB's Simscape environment is shown in Fig. 1.

The sheet resistance of the electrode is converted into the total resistance between one end of the electrode to the other using the following expression:

$$R = \frac{\rho L}{A} = \frac{R_s t L}{A}, \quad (3)$$

where  $R_s$  is the sheet resistance,  $\rho$  is the resistivity,  $A$  is the cross sectional area,  $t$  is the electrode thickness, and  $L$  is the length of the electrode. The resistance of each resistor in the RCR ladder is the total resistance as obtained in Equation 3 divided by the number of units in the RCR ladder. The capacitance of each capacitor is the total capacitance of the polymer film divided by the number of units in the RCR ladder. The total capacitance of the film is calculated by treating the

polymer as a parallel plate capacitor. The formula for the capacitance of a parallel plate capacitor is

$$C = \frac{\epsilon_o \epsilon_r A}{d}, \quad (4)$$

where  $\epsilon_o$  is the permittivity of free space,  $\epsilon_r$  is the permittivity of the polymer layer,  $A$  is the area of the electrode, and  $d$  is the distance between electrodes. The voltage is measured across the capacitor at the end of the ladder to determine the time taken to charge and discharge the slowest capacitor. If the actuator is subjected to a sinusoidal wave, the capacitive layer has to charge to a positive voltage, discharge to zero, charge to a negative voltage, and return to zero, presuming the time taken to complete a full wavelength will be equivalent to  $4 \times$  the time taken to charge the capacitive layer. This can be used to find the frequency at which the actuator can operate.

### III. RESULTS AND DISCUSSION

#### A. Manufacturing results

1) *JS-B25P on Novele*: The printer requires an approximate 5 printing runs to fully coat a sheet of Novele substrate at the highest CD print quality settings. The unsintered printed shapes were examined under an optical microscope (Keyence, VHX-6000) as well as a white light interferometer to determine the topography of the prints. Repeated printing runs of 2 to 3 layers still showed voids and holes where the deposited ink was not able to produce an consistent homogeneous coating. The printed samples are held up to a light to determine if there are any points through which light is visible. Four print cycles produced a homogeneous surface with occasional minor defects and 5 printing cycles produces a fully coated surface with no visible vacant spots through which the substrate or light was visible. The increase in surface coverage with increasing layers is shown in Fig. 2.

The topography measurements of the 5 print cycle samples (Fig. 3) show the silver particles form a sheet approximately 0.8-1  $\mu\text{m}$  thick, being slightly thicker around the edges than in the center. This variance in thickness is likely a result of the printing pattern, which unfortunately cannot be controlled with the consumer software available. The same variance in thickness of the printed layers was observed in samples printed on PEN and Kapton film substrates.

It was noted that after extended storage the printed samples with 2 and 3 layers would exhibit defects in the form of pockmarks which were initially nonexistent. Samples with 4 printing cycles and greater did not exhibit the same symptoms. It is possible this is due to the absorbent substrate drawing in moisture which results in a reaction with the silver. Samples with unexposed substrate would be less likely to draw in moisture and as such would not exhibit the same symptoms. When the pockmarks are examined under an optical microscope it is observable that the spots are discolored regions, rather than holes or deformations in the silver layer. Scans from a white light interferometer confirm that none the discolored regions differ topographically from the regions around them to any observable degree.

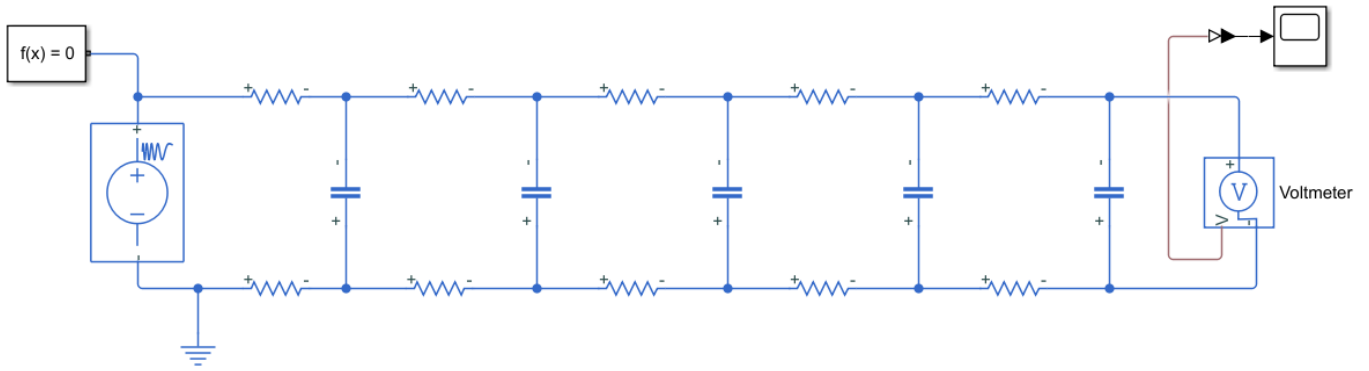


Fig. 1. RCR ladder simulation constructed in Simulink

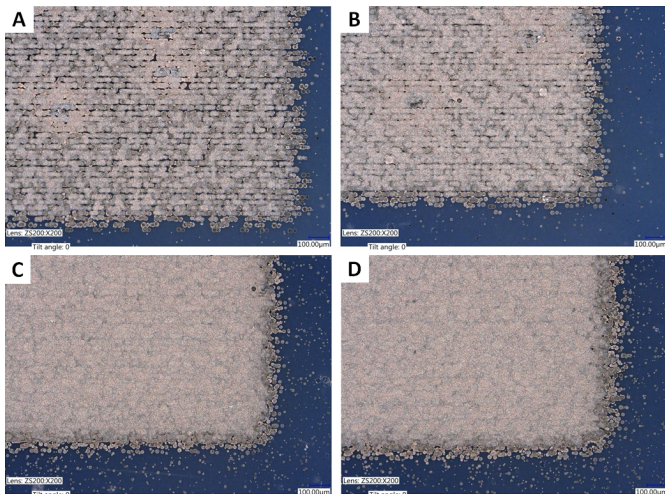


Fig. 2. Sintered JS-B25P silver ink printed on Novele: A. 2 layers B. 3 layers C. 4 layers D. 5 layers



Fig. 4. 5 layers of sintered JS-B25P silver ink printed on Novele

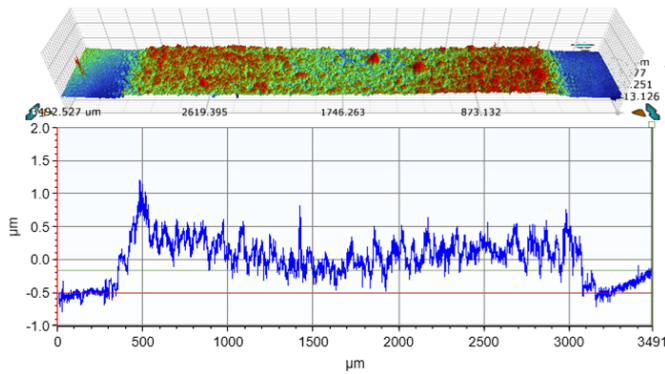


Fig. 3. Topography of 5 layer unsintered JS-B25P silver ink on Novele

After sintering the silver becomes a notably lighter color, going from a metallic grey to a light yellow tone. The best sintering results were achieved with 5 printed layers or above as shown in Fig. 4. The parameters in Table I are suited for sintering 5 layer samples on Novele, though the laser power should be increased to 80. If these same laser cutter parameters

are applied to samples with fewer printed layers, the sintering process will cause damage to the film and result in the silver flaking off and producing holes in the film as shown in Fig. 5. If used on samples with more than 5 printed layers, it will not adequately sinter the ink and not produce any significant increase in conductivity.

2) *JS-B25P on Kapton & PEN*: Due to an extreme sensitivity to surface defects and static, printing on Kapton and PEN film produces extremely inconsistent results, and requires 8-10 layers to be achieved semi-decent coverage. As the surface of Kapton and PEN films are non-absorbing, the deposited ink forms droplets on the surface and is dependent on wetting to spread and cover the surface. These plastic films also accrue static charge during manufacture and transport, and the presence of static appears to affect the trajectory of ink droplets during printing. Printing on samples with heavy static produced very inconsistent coating with regular voids and thicker regions where ink would accumulate. The best printed layer is achieved when covering the printing tray and CD with a solution of fabric softener and water, and allowing the residue to dry without wiping it off. The presence of a

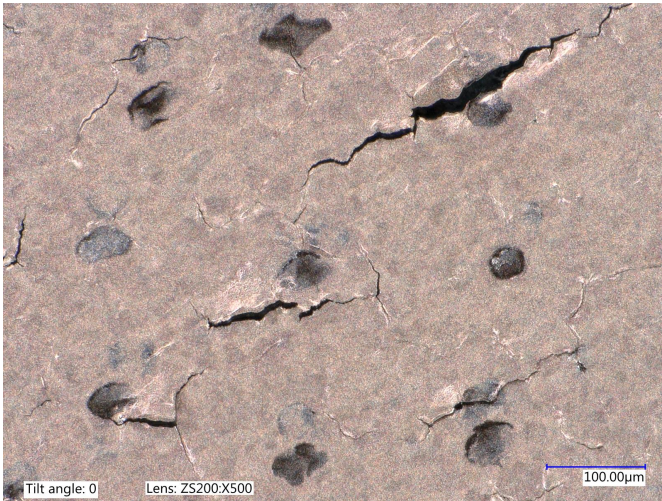


Fig. 5. 4 layers of sintered JS-B25P silver ink printed on Novele

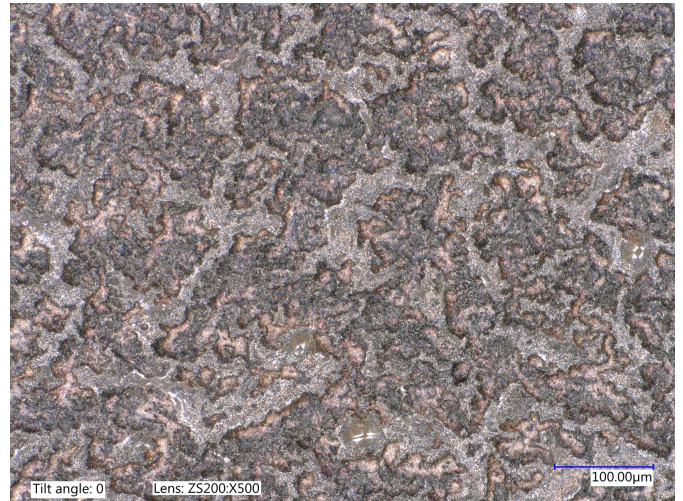


Fig. 7. 10 layers Under sintered JS-B25P silver ink printed on PEN

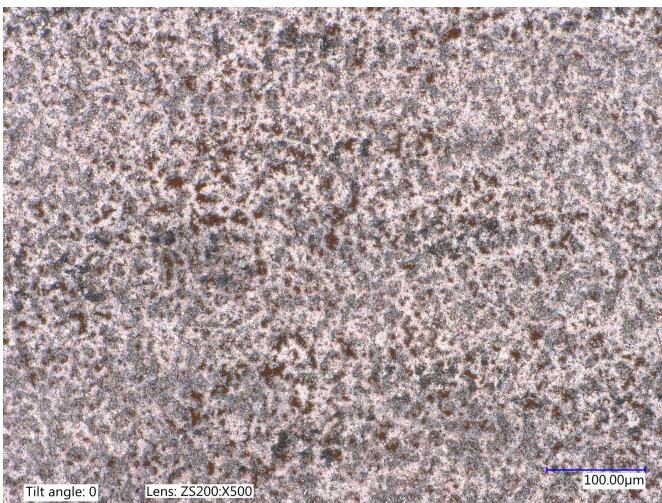


Fig. 6. 10 layers Sintered JS-B25P silver ink printed on Kapton

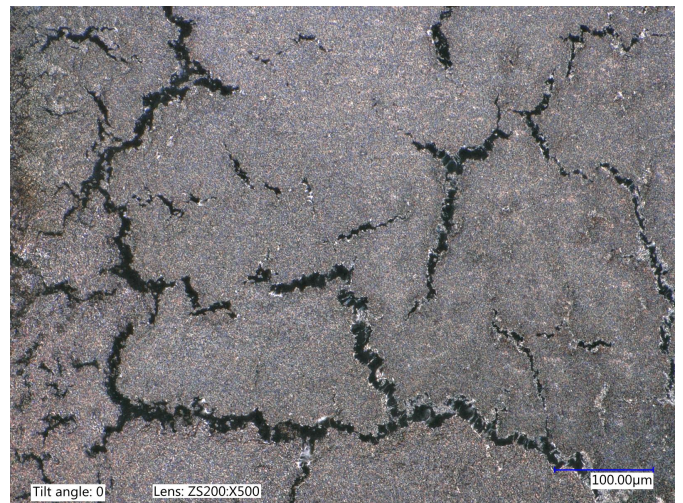


Fig. 8. 10 layers Over sintered of JS-B25P silver ink printed on PEN

surfactant layer left by the fabric softener helps reduce the amount of static on the surface. When preparing the film, it is essential to try and touch the surface of the film as little as possible. The film is submerged into a (5:1) solution of water to fabric softener, and blown dry. The film is then rinsed in propan-2-ol and blown dry. When attaching the film to the CD tray, tape must not be applied close to the regions where printing will take place, as the tape exhibits static and will affect the print. Lastly wipe the film down very gently with a cotton ball to remove any residue on the surface of the film. When preparing the film, any surface marks, however minute will have an effect on printing. Scratches or remaining residue will affect ink deposition and not produce even films. The surface of the printed ink will also be quite uneven, suffering from a noticeable orange peel effect. A possible solution for this is to treat the surface with oxygen plasma to induce a hydrophilic layer with improved ink wettability [5].

Once printed, the ink does not dry and retains its dark brown

color. Once sintered, the ink becomes a grey color. The degree of sintering depends on the amount of the ink and thickness of the ink layer. The great variation in ink deposition across the substrate means very uneven sintering with patches of lighter and darker silver, with corresponding large variations in conductivity. The printing parameters as described in Table I function well for Kapton, which can take relatively high laser power without damage (Kapton is thermally stable until 400°C). Sintered samples printed on Kapton are shown in Fig. 6. Sintering PEN samples however presents a significant challenge. Laser settings which fully sinter the silver heat up the substrate and cause deformation in the PEN layer, breaking the silver film and causing cracks (Fig. 8). Laser powers set low enough to not damage the substrate will not sinter the silver and produce lackluster conductivity (Fig. 7).

3) *JR-700LV on Novele*: The carbon black nanoparticle ink produces a matte coating compared to other inks, making it more difficult to observe defects or variances in film thickness

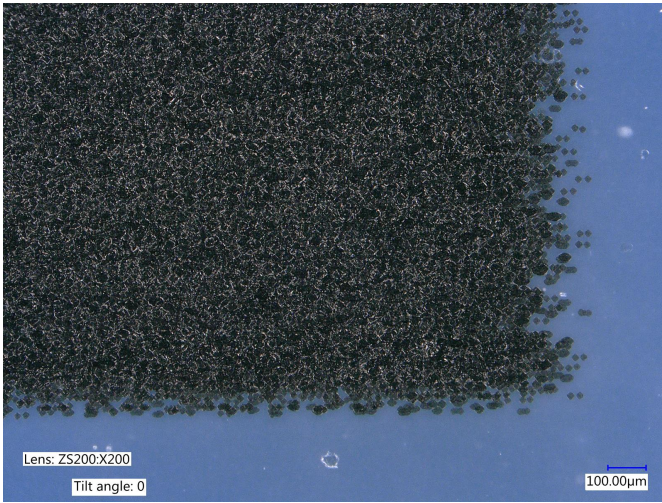


Fig. 9. 6 layers of JR-700LV carbon black ink printed on Novele

with the optical microscopy. The light absorption of the carbon black particles also make it difficult to measure using white light interferometry. Due to the lower solid material content of the carbon ink, 6 or more printed layers are required to produce full even coverage of the substrate with no voids (Fig. 9).

4) *JR-700LV Kapton & PEN*: The carbon black contains a 3.5% weighting, significantly lower than the silver or the copper inks. As such, the ink appears to be much more fluid and is affected more by surface tension of the fluid the particles are suspended in. When printing on Kapton or PEN film, the ink will occasionally not deposit at certain spots of the substrate, creating pinholes through which the substrate is exposed. Due to the fluid nature of this ink, the surface of the printed layer can be coaxed with a needle to cover the void. If the printed ink is sufficiently thick, once coaxed the ink will fully cover the hole and produce an entirely smooth surface. This is not possible with the silver ink, which is considerably more viscous and behaves similar to a paste.

5) *ICI-003 on Novele*: The ink deposited evenly and similarly to the silver and carbon inks, though showed no conductivity when freshly printed. Samples with 5 and 10 printed layers were produced and both sintered using the laser at a variety of different parameters. Sintered samples are shown in Fig. 10. All attempts to sinter the ink did not produce any measurable conductivity. As such this ink was not tested on any other substrates.

6) *NBSIJ-MU01 on Novele*: This ink was tested only on Novele substrate as it functions through chemical self sintering, and will only do so if printed on the appropriate substrate. The ink deposited very evenly and achieved full coverage with 5 layers. This ink produced a mirror sheen immediately after printing in contrast to the matte JS-B25P. As such it is safe to assume that whilst the JS-B25P similarly produced conductivity on Novele substrate without sintering, the formulation of these 2 inks do indeed differ. This ink does not suffer from the same pockmarks that arose with time in the

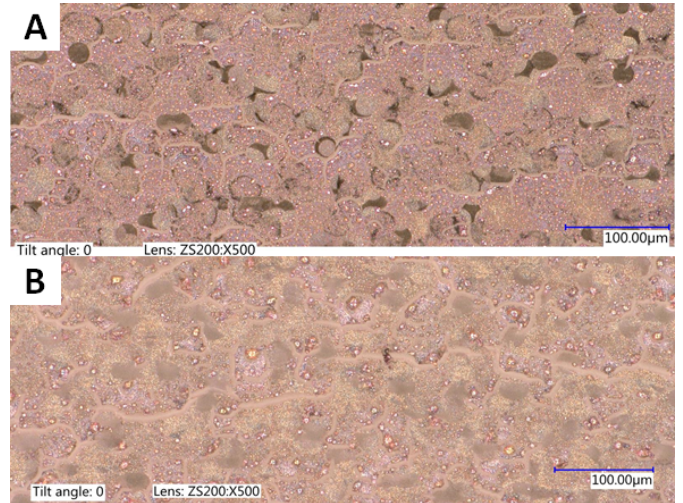


Fig. 10. Sintered copper on Novele: A. 5 layers B. 10 layers

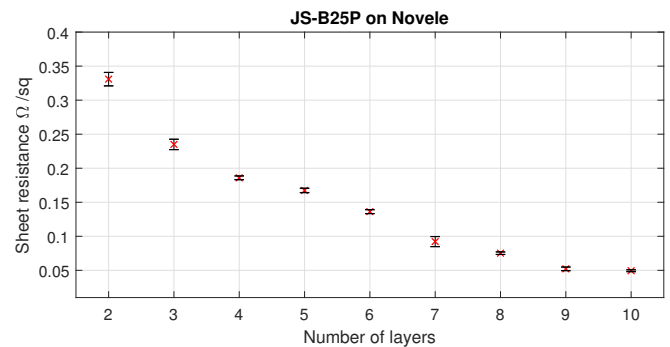


Fig. 11. Conductivity of JS-B25P silver ink printed on Novele

JS-B25P, and its appearance remains unchanged after months.

### B. Conductivity results

1) *Novele substrate*: The silver inks already produce conductivity with 1 printed layer, though the sheet resistance is very significantly higher than the resistance of samples with 2 or more layers. The sheet resistance also varies greatly across the printed region with a singular layer. Carbon black inks only show conductivity from 2 printed layers or more. As such the sheet resistance of single printed layers is omitted and instead results of 2-10 printed layers are plotted to better represent the data. A total of 10 resistivity readings are taken for each sample, and averaged. The conductivity of JS-B25P silver ink printed on Novele is shown in Fig. 11, JR-700LV carbon black ink printed on Novele is shown in Fig. 12, and NBSIJ-MU01 self sintering silver ink printed on Novele is shown in Fig. 13. The crosses represent the average sheet resistance, and the error bars represent the standard deviation. A comparison between sintered and unsintered samples of JS-B25P printed on Novele is shown in Table II.

The sheet resistance initially drops very significantly from 2-4 printer layers, with diminishing improvements in conductivity with additional layers from 5 layers and above. The

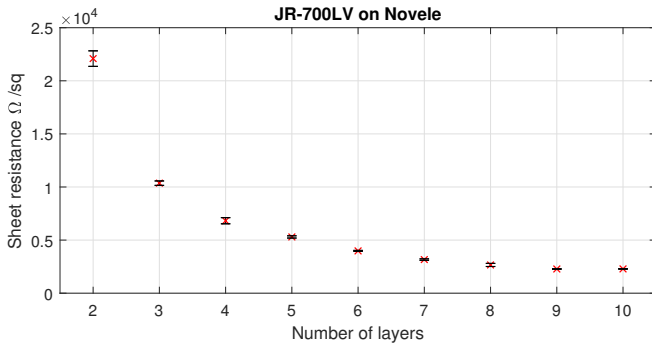


Fig. 12. Conductivity of JR-700LV carbon black ink printed on Novele

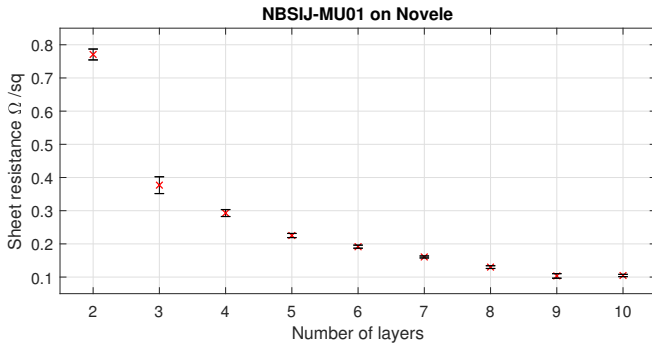


Fig. 13. Conductivity of NBSIJ-MU01 self sintering silver ink printed on Novele

standard deviation in sheet resistance of the samples also decreases, as shown by the shrinking error bars with increasing number of printed layers.

2) *PEN and Kapton substrates*: Samples printed on PEN and Kapton substrates will remain wet indefinitely and as such are nonconductive before drying or sintering. The sintered silver samples show increased sheet resistance on PEN and Kapton films compared to samples on Novele. Carbon black samples possess similar sheet resistance regardless of substrate. A comparison of conductivities is shown in Table III.

TABLE II  
AVERAGE SHEET RESISTANCE ( $\Omega/\square$ ) OF SINTERED VS UNSINTERED JS-B25P ON NOVELE

Ink	4 layers	5 layers	6 layers
Unsintered	0.1674	0.1362	0.0923
Sintered	0.1379	0.1003	0.0857
Percentage improvement	17.62%	26.36%	7.15%

### C. Modelling results

The actuators were manufactured in the form of cantilever beams as shown in the previous paper, with bottom electrode size  $3 \times 18$  mm, and top electrode size  $2.7 \times 17.5$  mm. The bottom electrode is made of 6 printed layers and the top electrode is made of 10 layers. Samples with 5 layers have a measured thickness of  $0.8\text{-}1 \mu\text{m}$  as shown in Fig. 3. Based

TABLE III  
AVERAGE SHEET RESISTANCE ( $\Omega/\square$ ) AND STANDARD DEVIATION OF 10 LAYER SAMPLES ACROSS DIFFERENT SUBSTRATES

Ink	Novele	PEN	Kapton
JS-B25P	$4.950(139) \times 10^{-2}$	$2.56(307) \times 10^3$	1.060(253)
JR-700LV	$2.2880(28.1) \times 10^3$	$2.0983(973) \times 10^3$	$2.151(131) \times 10^3$
NBSIJ-MU01	$1.0500(344) \times 10^{-1}$	n/a	n/a

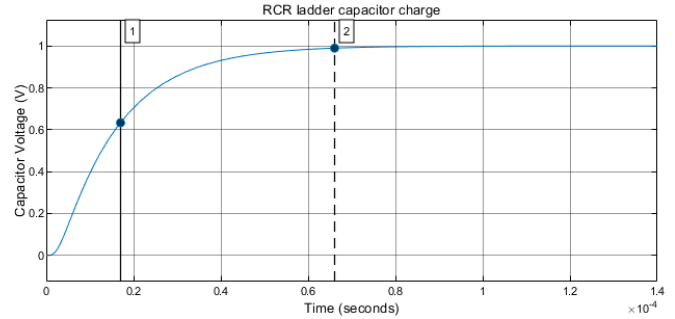


Fig. 14. Voltage of the fifth capacitor from the power supply with respect to time. 1. 63.2% charge, 2. 99% charge

on this, the bottom electrode is assumed to have a thickness of  $1 \mu\text{m}$  and the top electrode  $2 \mu\text{m}$ . The cross sectional area of the bottom electrode in  $\text{mm}^2$  is  $3 \times 0.001$  and the top electrode is  $2.7 \times 0.002$ . The length of the bottom electrode is 18 mm, and the top electrode 17.5 mm. As the bottom electrode consists of 6 layers of carbon black printed on Novele, the experimentally determined sheet resistance of  $3164.6 \Omega\text{m}$  is used (Fig. 12). The top electrode consists of 10 layers of carbon black printed on nonabsorbent P(VDF-TrFE-CTFE) polymer. As an approximation, the sheet resistance used is the average of the experimentally determined sheet resistances of 10 layer carbon black samples printed on nonabsorbent Kapton and PEN films (Table III).

The capacitance of the polymer layer is calculated using the area of the smaller top electrode as the area of the capacitive plate ( $A = 2.7 \times 17.5$  mm). The permittivity of free space is  $\epsilon_0 = 8.854 \times 10^{-12} \text{ Fm}^{-1}$  and the average relative permittivity  $\epsilon_r$  of the polymer layer is 45 [6]. The distance between the electrodes is equal to the thickness of the polymer layer, which is measured to be  $22 \mu\text{m}$ .

Substituting these values into the resistors and capacitors in the RCR ladder and applying 1 V DC gives the electrical behavior of the circuit. The time charging characteristic of the tip capacitor is shown in Fig. 14.

The RC time constant  $\tau$  (time taken to charge to 63.2% of applied DC voltage) is  $1.70 \times 10^{-5}$  s, and the time taken to reach 99% charge is  $6.61 \times 10^{-5}$  s as marked by the cursors on Fig. 14. Assuming the actuator is subjected to a sinusoidal input and a full sinusoid requires a total of 4 charging/discharging cycles, the capacitive layer will have to charge to a positive voltage, discharge to 0, charge to a negative voltage, and discharge to 0. The fastest time the capacitor can achieve this with whilst charging to 63.2% is



$4 \times 1.70 \times 10^{-5} = 0.068$  ms and to 99% charge is  $4 \times 6.61 \times 10^{-5} = 0.2644$  ms. This corresponds to a frequency of 14.705 kHz and 3.782 kHz respectively.

#### D. Discussion

The sheet resistances of all 2 layer samples printed on Novele are significantly larger than samples with 3 layers or more. This sudden and significant decrease in sheet resistance is likely due to the 2 layered samples not having enough conductive particles to form consistent connections across the printed region. This also explains the greater standard deviation in sheet resistance readings for 2 layer samples.

The datasheet for JS-B25P silver ink reports a sheet resistance of 60-70  $m\Omega/\square$  after photonic sintering, if printed on Novele substrate [7]. The sheet resistance we achieved for 5 layer laser sintered samples on Novele was 100.3  $m\Omega/\square$ , showing a reasonable degree of similarity. The similarity of the sheet resistances we obtained compared to the results reported in the datasheet in addition to the demonstrated improvement in the conductivity of sintered silver samples compared to unsintered samples shows the viability of laser sintering as performed in this paper. Printing additional layers showed a reduction in sheet resistance down to 50  $m\Omega/\square$  for 10 layered unsintered samples, outperforming the values presented in the datasheet. Given that the datasheet gives no information on how many layers are printed at what settings, it is difficult to determine if these results are an anomaly or simply the expected result of adding a very large volume of silver particles.

Using NBSIJ-MU01 silver ink, Kawahara et al. achieved 0.19  $\Omega/\square$  when printing on porous resin coated PET films similar to Novele [8]. The method of manufacture used by Kawahara et al. differed slightly as a different model of printer was used and samples were printed using a normal paper printing tray. Based on observation, the printing settings for paper and CDs differ significantly in the maximum volume of ink that can be dispensed, with settings for printing on paper depositing significantly more ink than when printing on CDs. The range of sheet resistances of NBSIJ-MU01 self sintering silver ink as we identified in this paper are however comparable with reported values in literature, and show good coherence.

Whilst no literature exists on the conductivity of JR-700LV carbon black ink, Schlatter et al. produced similar inkjet printable carbon black inks for use with dielectric elastomer actuators [9]. The samples were printed using an industrial inkjet printer, and produced films 1-1.08  $\mu\text{m}$  thick after 2 layers with a sheet resistance of 13  $k\Omega/\square$ . Due to the very different ink formulation as well as printing parameters, the exact resistances cannot be expected to match exactly. The results we obtained with printed carbon black differed by an order of magnitude, suggesting a marginal degree of similarity.

The failure to properly sinter the copper was not unexpected, as silver nanoparticles require either a broad spectrum light source such as a xenon bulb or a laser specifically in the 808-1064 nm wavelength region to properly sinter [10]. The

laser in the Micro laser etching machine operates at a 355nm wavelength. Whilst copper is expected to have the benefit of better conductivity than carbon black at the same price point, the need for special equipment somewhat diminishes this advantage.

The advantage of carbon black over silver nanoparticles was initially expected to be the lack of post processing required. It was believed that the non self sintering silver ink (JS-B25P) would not produce conductivity without sintering, but given that the silver ink can produce instantaneous conductivity without post processing on Novele substrate, the lack of post processing required for carbon black inks no longer becomes an advantage over other inks when printing on Novele substrates. Carbon however only requires drying when printed on PEN and Kapton films, whilst silver ink requires sintering. Thus the lack of post processing is still an advantage when used on nonabsorbent substrates. Another advantage of carbon black over silver nanoparticles is flexibility and fatigue resistance, with carbon electrodes contributing negligibly to the effective stiffness of actuators [11]. The significantly lower price of carbon black compared to silver nanoparticles remains a point of interest, although the price is identical to that of copper nanoparticle inks. As such carbon black may be better suited for applications requiring low temperature processing rather than applications desiring highly conductive materials.

P(VDF-TrFE-CTFE) actuators previously produced at TU Delft used 20 nm thick electrodes made using spin coated gold. If the resistivity of the electrodes is assumed to be the same as bulk gold ( $2.44 \times 10^{-8} \Omega\text{m}$ ), the sheet resistance is calculated to be 1.22  $\Omega/\square$ . This is a very similar resistance to what is achievable using both JS-B25P and NBSIJ-MU01 silver inks, though the thickness of the silver films is considerably greater. As the modelling shows, it is possible to achieve operation up to 3.782 kHz using carbon black inks to produce the electrodes. The use of more conductive electrodes will increase the frequency at which an actuator can operate, though they will not improve the deflection. As such carbon black is a perfectly suitable electrode material unless higher frequency operation is desired. The use of certain electrode materials such as sintered silver ink would increase the stiffness of the cantilever beam and actually reduce actuator deflection.

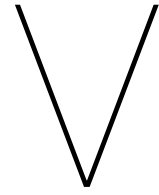
#### IV. CONCLUSIONS

The conductive performance of a number of inkjet printable nanoparticle dispersions are demonstrated across a range of substrates. The best conductivities were achieved when printing on a microporous resin coated PET substrate (Novele IJ-220, Novacentrix), which also produced instantaneous conductivity without the need for additional drying or post processing. The lowest resistances were achieved using 25% loading silver nanoparticle ink, and the worst results yielding the lowest conductivity were produced from carbon black nanoparticle ink. When printing on nonabsorbent substrates, carbon black required the least post processing to become conductive compared to silver inks which required either intensive thermal or photonic sintering. Photonic sintering

performed using a laser improved conductivity of silver inks but was not compatible with all substrates and could quite easily damage the underlying material. Modelling of a P(VDF-TrFE-CTFE) actuator showed that despite high resistance, carbon black could be used as an electrode material in and still achieve 99% of maximum deflection when operating up to 3.782 kHz. This demonstrates the suitability of carbon black inks for use as electrodes in temperature sensitive ferroelectric polymer actuators.

#### REFERENCES

- [1] 2011, "Data Sheet: Novele IJ-220". [Online]. Available: [https://store.novacentrix.com/v/vspfiles/assets/images/novele%20ij-220\\_2212.2.pdf](https://store.novacentrix.com/v/vspfiles/assets/images/novele%20ij-220_2212.2.pdf)
- [2] "Pen film - Material information". [Online]. Available: <http://www.goodfellow.com/E/Polyethylene-naphthalate-Film.html>
- [3] 2018, "Data Sheet: Kapton HN". [Online]. Available: <https://www.dupont.com/content/dam/dupont/products-and-services/membranes-and-films/polyimide-films/documents/DEC-Kapton-HN-datasheet.pdf>
- [4] H. Topsoe, *Geometric factors in four point resistivity measurement*, 1968.
- [5] S. Yuichi, F. Tomoaki, and A. Masatoshi, "Preparation of batio 3 thick films by inkjet printing on oxygen-plasma-modified substrates," *Japanese Journal of Applied Physics*, vol. 45, no. 9S, p. 7247, 2006.
- [6] 2018, "Technical Data Sheet: TDS PIEZOTECH RT-TS". [Online]. Available: <https://www.piezotech.eu/en/Technical-center/Documentation/>
- [7] 2016, "Data Sheet: MetalonJS-B25P". [Online]. Available: [https://www.novacentrix.com/sites/default/files/pdf/Metalon%20JS-B25P\\_1.pdf](https://www.novacentrix.com/sites/default/files/pdf/Metalon%20JS-B25P_1.pdf)
- [8] Y. Kawahara, S. Hodges, B. S. Cook, C. Zhang, and G. D. Abowd, "Instant inkjet circuits: lab-based inkjet printing to support rapid prototyping of ubicomp devices," in *Proceedings of the 2013 ACM international joint conference on Pervasive and ubiquitous computing*. 2493486: ACM, Conference Proceedings, pp. 363–372.
- [9] S. Schlatter, S. Rosset, and H. Shea, "Inkjet printing of carbon black electrodes for dielectric elastomer actuators," in *SPIE Smart Structures and Materials + Nondestructive Evaluation and Health Monitoring*, vol. 10163. SPIE, Conference Proceedings, p. 9.
- [10] 2017, "Data Sheet: CI-004". [Online]. Available: [http://intrinsicmaterials.com/wp-content/uploads/2018/04/CI-004\\_Data\\_Sheet\\_2017\\_v1.3.pdf](http://intrinsicmaterials.com/wp-content/uploads/2018/04/CI-004_Data_Sheet_2017_v1.3.pdf)
- [11] C. A. d. Saint-Aubin, S. Rosset, S. Schlatter, and H. Shea, "High-cycle electromechanical aging of dielectric elastomer actuators with carbon-based electrodes," *Smart Materials and Structures*, vol. 27, no. 7, p. 074002, 2018.



## Conclusions

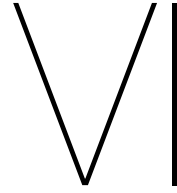
This thesis proves the viability of inkjet printed carbon black electrodes for use with P(VDF-TrFE-CTFE) ferroelectric polymer actuators. This opens the way for inkjet printed actuators with performance and ease of manufacture not previously possible. The actuators produced notably outperform similar inkjet printed actuators produced from P(VDF-TrFE). To achieve this, first a literature study was performed to form a foundation as to what inkjet printed sensors and actuators exist, as well as what efforts have been done to print other smart materials.

The literature study identifies a number of inkjet printed sensors and actuators, and highlights a number of early efforts into printing various active materials. Literature consistently indicates the simplicity of printing polymers compared to other active materials such as piezoelectric ceramics. A number of papers demonstrate the possibility of fully inkjet printed ferroelectric polymer actuators, wherein both the electrodes and active polymer material are deposited using inkjet printing. Existing fully inkjet printed actuators all use P(VDF-TrFE) with silver electrodes. Silver electrodes require post processing to become conductive and contribute to the effective stiffness of the actuator. In contrast to this, carbon black electrodes require no post processing and contribute negligibly to the stiffness of actuators. The terpolymer P(VDF-TrFE-CTFE) produces greater strains than P(VDF-TrFE), and can be used to produce actuators with greater deflection. As such, carbon black electrodes and P(VDF-TrFE-CTFE) both showed potential for use to produce actuators with greater strain and ease of manufacturing than previously possible.

The conference paper demonstrates the manufacture of novel relaxor ferroelectric polymer actuators by utilizing inkjet printed carbon black electrodes. Such ferroelectric actuators using inkjet printed carbon black electrodes have not been attempted before, and no other P(VDF-TrFE-CTFE) actuators using inkjet printed electrodes currently exist. The methodology employed uses a commercial inkjet printer and allows for the manufacture of ferroelectric polymer actuators to be done much cheaper and faster than previously possible. The produced actuators were able to achieve  $206\ \mu\text{m}$  steady state deflections at 300 V and over 3 mm at resonance. This shows a 42% improvement in steady state deflection, and a 89.4% improvement in strain per volt compared to similar inkjet manufactured P(VDF-TrFE) actuators with silver electrodes in literature [4].

The supplementary paper provided the necessary basis for the material selection and construction of the actuator. This report summarizes the conductive performance of silver, carbon black, and copper nanoparticle inks as printed with a commercial printer. Silver inks were found to produce the lowest resistance, achieving  $50\ \text{m}\Omega/\square$  after 10 printed layers on a resin coated PET substrate (Novole). When silver inks were printed on nonabsorbing polymer substrates, no conductivity could be produced until photonic sintering. The quality of ink deposition and conductivity after sintering was inconsistent and unreliable. Carbon black inks became conductive after simply drying at low temperatures, and electrodes could

be manufactured much faster and with fewer steps. Modelling showed that despite the higher resistivity of carbon black, electrodes made of carbon black could still allow for actuator operation up to 3.782 kHz and achieve 99% of maximum deflection.



## Reflections and Recommendations

Attempts were made to print the polymer layer using a blend of MEK/DMSO and 0.5-1 wt% of P(VDF-TrFE-CTFE), however the commercial printer used failed to deposit the ink regardless of polymer content. The MEK/DMSO mixture itself was printable, indicating the issue stemmed from the inclusion of the polymer rather than incompatibility of the solvents with the printer. The polymer solution was observed to solidify rapidly in contact with any water, meaning that the presence of any moisture in the printhead would instantly lead to clogging. As the printer came from the factory with ink residue inside the printheads, it was extremely difficult to fully dry out the internal channels of the printhead. This is likely the cause of failure. However given that the most time consuming step of actuator manufacture is the production of electrodes rather than the polymer layer, the printing of the electrodes was of greater importance than the printing of the polymer. Given that 3 spin coated layers of polymer was required to produce full insulation between the electrodes, inkjet printing the polymer layer could actually require longer than spin coating as the volume of ink deposited would have to be much greater due to the significantly lower polymer content.

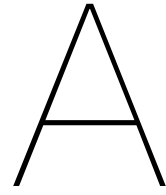
The time taken to manufacture a set of 8 actuators is 4 hrs, as compared to the 5 hrs required by research done previously at TU Delft [7] (As verbally conveyed by the supervisor). The methodology used previously required manufacturing in a clean room and did not consistently produce functioning actuators. This increased the manufacturing time beyond the time required for purely the manufacturing steps.

The sheet resistances achieved by the inkjet printed films and the deflections achieved by the actuators show highly satisfactory results, and indicate an improvement over what has so far been achieved in literature. There remains great potential for further research in the field of inkjet printed sensors and actuators, with several areas that can be improved.

- Inkjet printed polymer layer: The polymer layer can be produced using inkjet printing rather than spin coating. Through a mix of DMSO/MEK it is possible to render P(VDF-TrFE) into an inkjet printable ink [5]. Alternatively triethyl phosphate is a proven solvent suitable for rendering P(VDF-TrFE-CTFE) into an inkjet printable ink [6]. Further work should investigate if this same solvent mix produces a P(VDF-TrFE-CTFE) ink printable with a commercial inkjet printer.
- Carbon nanotube electrodes: The carbon black electrodes can be replaced with multi-wall carbon nanotubes. Such conductive inks in literature show improved conductivity over similar carbon black inks whilst also requiring no post processing beyond drying [8].
- Treated Kapton/PEN films: Coating a substrate with ethyl cellulose and treating this layer with oxygen plasma has been shown to induce hydrophilic properties in the surface, improving wettability and vastly improving even ink deposition. This has the po-

tential to resolve the ink deposition issues on nonabsorbent Kapton and PEN substrates [9].

- **Multilayer structure:** The beam could be transformed from a unimorph beam into a bimorph beam by printing another active layer on top of the existing layer or on the underside. Given the good deposition of carbon black inks on nonabsorbing substrates, this would require no alternation in materials or methodology used. The second layer could be used to improve actuation or instead act as a sensing layer [10].
- **Intense pulsed light sintering:** If intense pulsed light was used instead of a laser for photonic sintering, it would be easier to achieve even sintering without damaging sensitive polymer substrates such as PEN film [11]. This would also allow for the sintering of copper [12]. This would allow copper to be used as an electrode material, with the potential of granting improved conductivity over carbon black whilst remaining at the same price point.
- **Flexures:** The actuators in this paper can be used as controllable flexures or to form active resonators to dampen flexures. A large network of printed actuators can be used to achieve distributed actuation. The difficulty associated with this is that the printer can only print on flat films, and cannot produce 3D structures. The construction of 3D structures would require the actuators to first be printed as flat films and then manually assembled, or require kirigami type structures [13].



# Manufacturing Steps






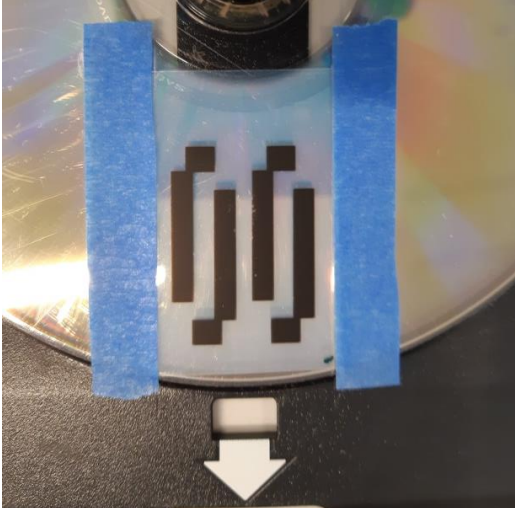

Image	Process step	Notes
	<p>Cut a 25x40mm piece of Novele substrate and attach it to the CD mounted to the CD printing tray. Place the substrate above or below the CD hole, horizontally centered with respect to the CD printing tray.</p>	
	<p>Using the Epson Print CD software, print the bottom electrode using Print Color Correction +3 and media type: CD/DVD Premium Surface. Repeat printing the desired number of times until the substrate is satisfactorily coated. Carbon black bottom electrodes require 6 layers.</p>	<p>The printing procedure is the same as used for printing on a CD normally. Follow the prompts on the printer screen for when to insert the tray.</p>
	<p>Dry the bottom electrode in an oven at 80 °C for 30 mins.</p>	<p>Tape the substrate down to a petri dish to avoid curling.</p>

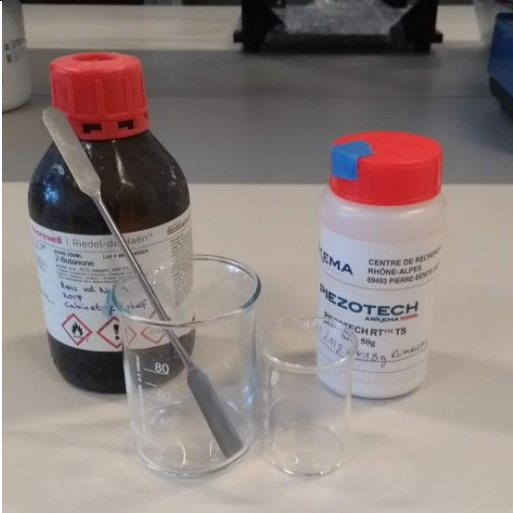

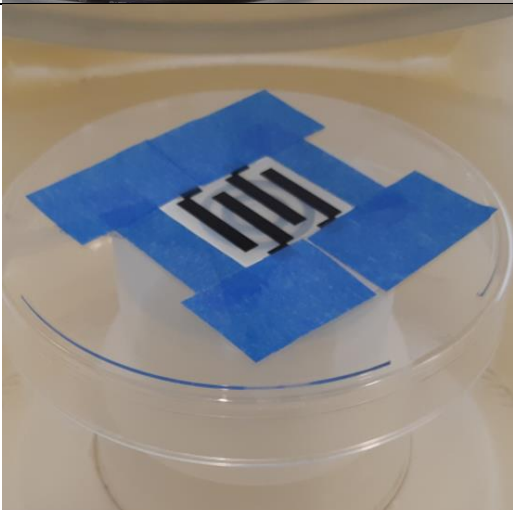
Image	Process step	Notes
	<p>Mix polymer with MEK at a ratio of 10:1 (MEK to P(VDF-TrFE-CTFE)), mix until homogenous.</p>	<p>The solvent continually evaporates and the solution becomes thicker, so the mixing and spin coating procedure should be done as quickly as possible.</p>
	<p>Place polymer solution in dessicator to remove bubbles.</p>	<p>Bubbles in the spin coated polymer layer will cause short circuits between the electrodes.</p>
	<p>Mount the substrate to the underside of a petri dish and mask the electrode contact pads with glass slips held down firmly with tape. This prevents the contact points from being coated with polymer. Place the petri dish in the spin coater.</p>	<p>The glass slips have to be as flush with the substrate as possible to prevent polymer seeping underneath.</p>

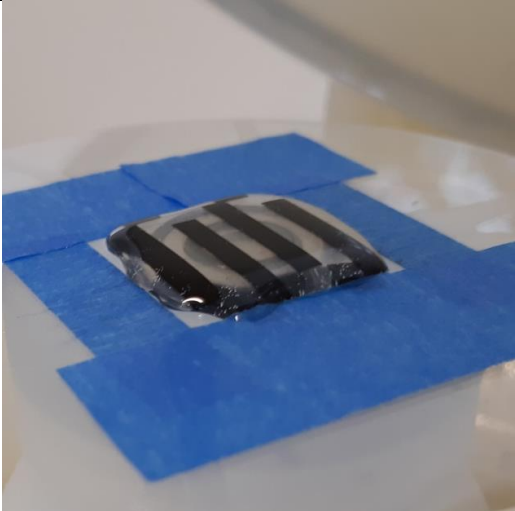
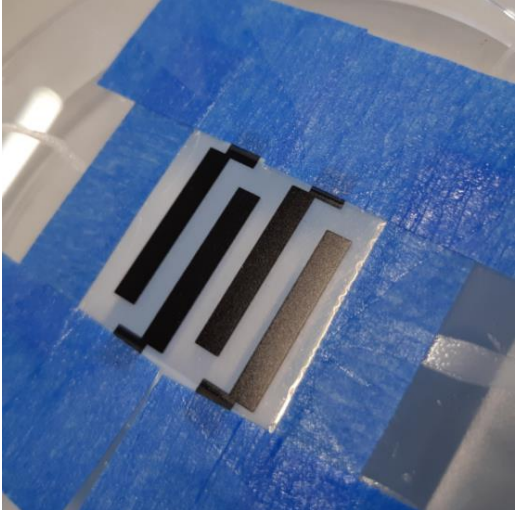
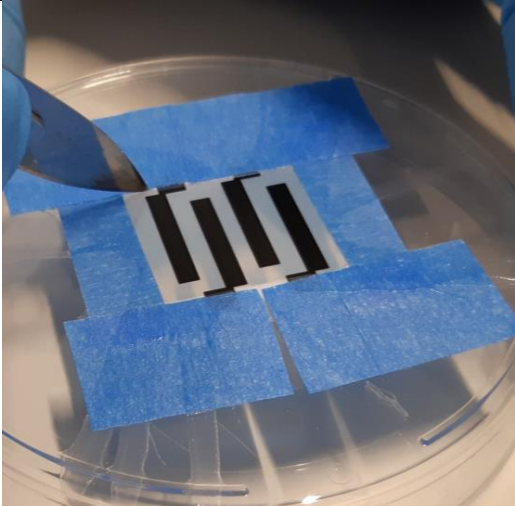
Image	Process step	Notes
	<p>Pour enough polymer solution to cover the bottom electrodes. Spin coat at 1500 rpm with 150 rpm/s acceleration for 30 s.</p>	<p>Due to the absorptive behavior of the substrate, the polymer will have difficulty spreading to regions it was not poured on to begin with.</p>
	<p>Allow the spin coated layer to air dry for 1 minute, before repeating the spin coating process another 2 times to produce a total of 3 polymer layers.</p>	<p>The polymer will lose its sheen when dry, and become matte.</p>
	<p>Remove the tape and glass slips masking the electrode contact pads. A slight incision at the edge of the mask is useful to make sure the tape does not peel the polymer layer off along with it.</p>	<p>Be extremely gentle when removing the masking tape.</p>


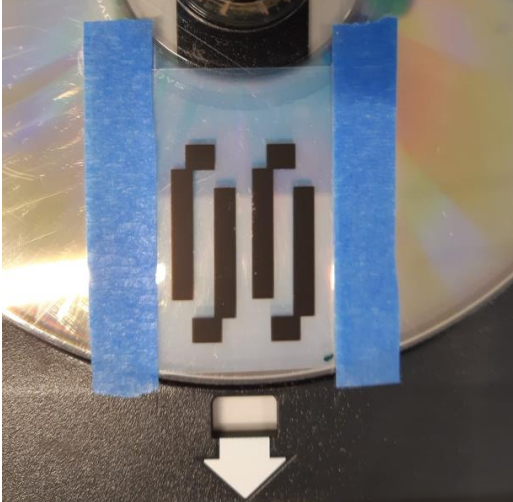

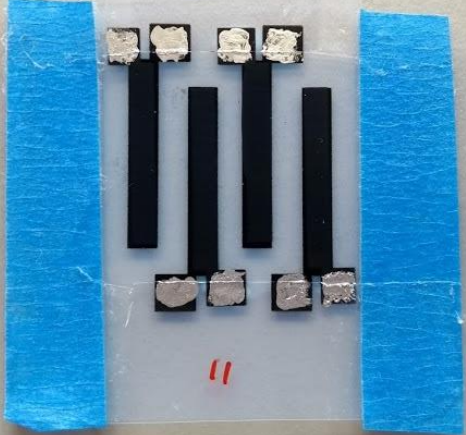

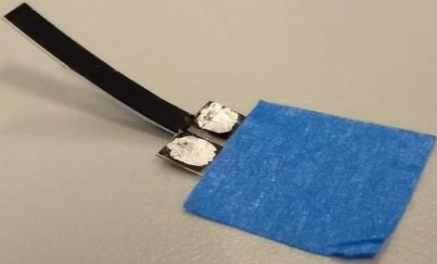
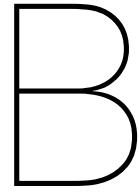
Image	Process step	Notes
	<p>Sinter the sample in an oven at 111 °C for 2 hrs.</p>	<p>The temperature must be above the polymer annealing temperature of 110 °C and below the melting temperature of 120 °C.</p>
	<p>Mount the sample to the CD printing tray as before and using the Epson Print CD software, print the top electrode using Print Color Correction +3 and media type: CD/DVD Premium Surface. Repeat the desired number of times until the substrate is satisfactorily coated. Carbon black top electrodes require 8-10 layers.</p>	<p>Make sure to position the top electrodes on top of the bottom electrodes.</p>
	<p>Dry the top electrode in an oven at 80 °C for 30 mins.</p>	<p>Depending on the number of printed layers, drying may take more than 30 mins. The electrode is dry when it achieves an even matte finish.</p>

Image	Process step	Notes
	<p>Apply silver paint at the contacts to improve contact.</p>	
	<p>Pole the sample by applying 140 V DC to the electrodes, whilst heating to 85 °C for 25 mins. After 25 mins, Remove the heat source whilst maintaining 140V DC until sample reaches room temperature. Remove the voltage source once cooled.</p>	<p>The heating increases the conductivity between the electrodes and may cause a short circuit through the polymer layer. The poling process will typically cause defective actuators to fail. Monitor samples carefully to determine if actuators spark or short circuit.</p>
	<p>Cut out the actuator using a scalpel. The actuator is now ready for use.</p>	<p>Due to the thermal treatments, the cantilever will curl slightly. This does not affect performance.</p>





## Electrode Patterns

Attached are the image files used in the Epson Print CD software to print the electrodes. The images are imported and superimposed on a CD surface in the software, using default scaling. The patterns are designed to deposit ink in the regions where the substrate is mounted as described in Appendix A.





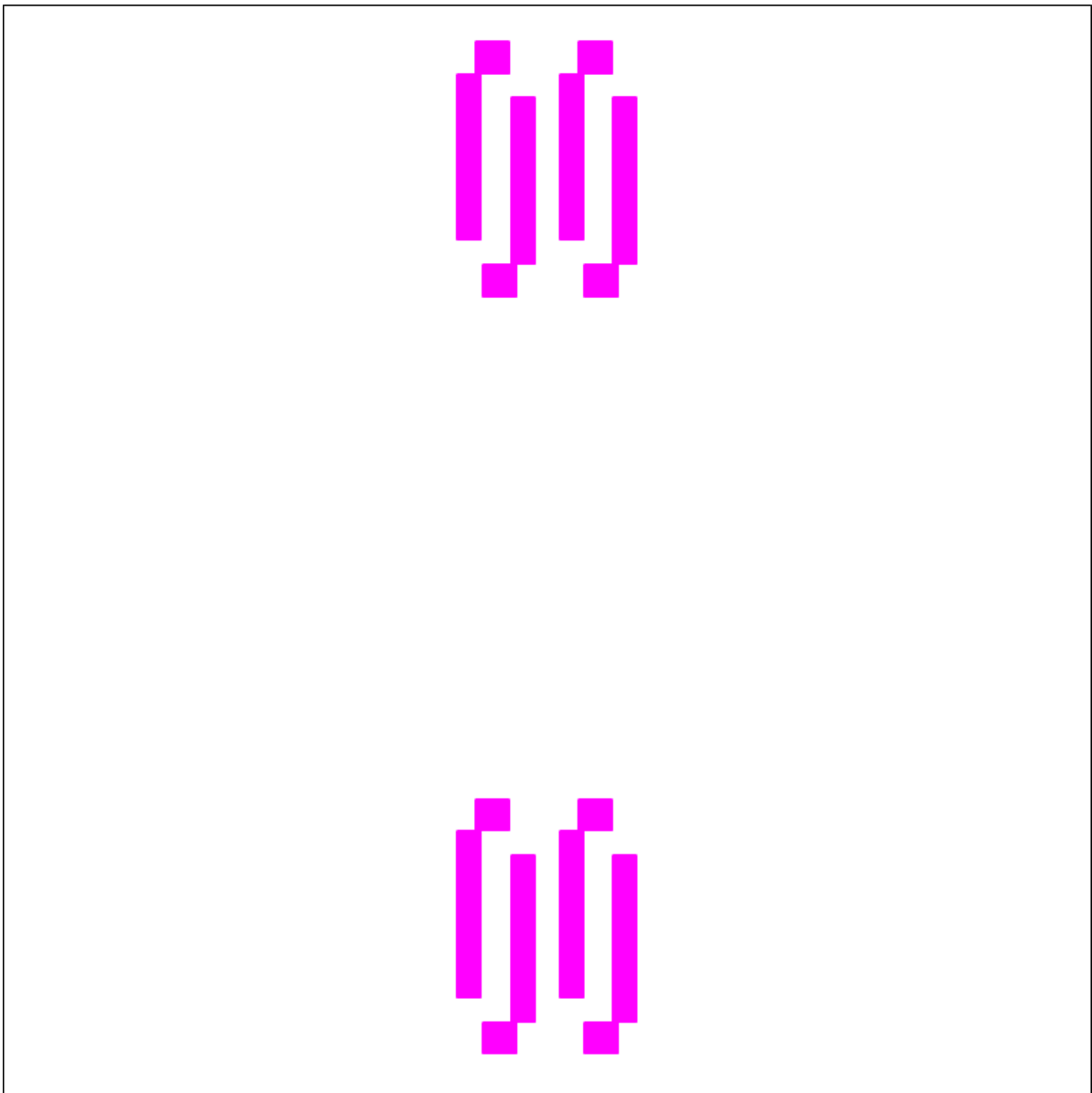


Figure B.1: Image used in Epson Print CD for bottom electrode

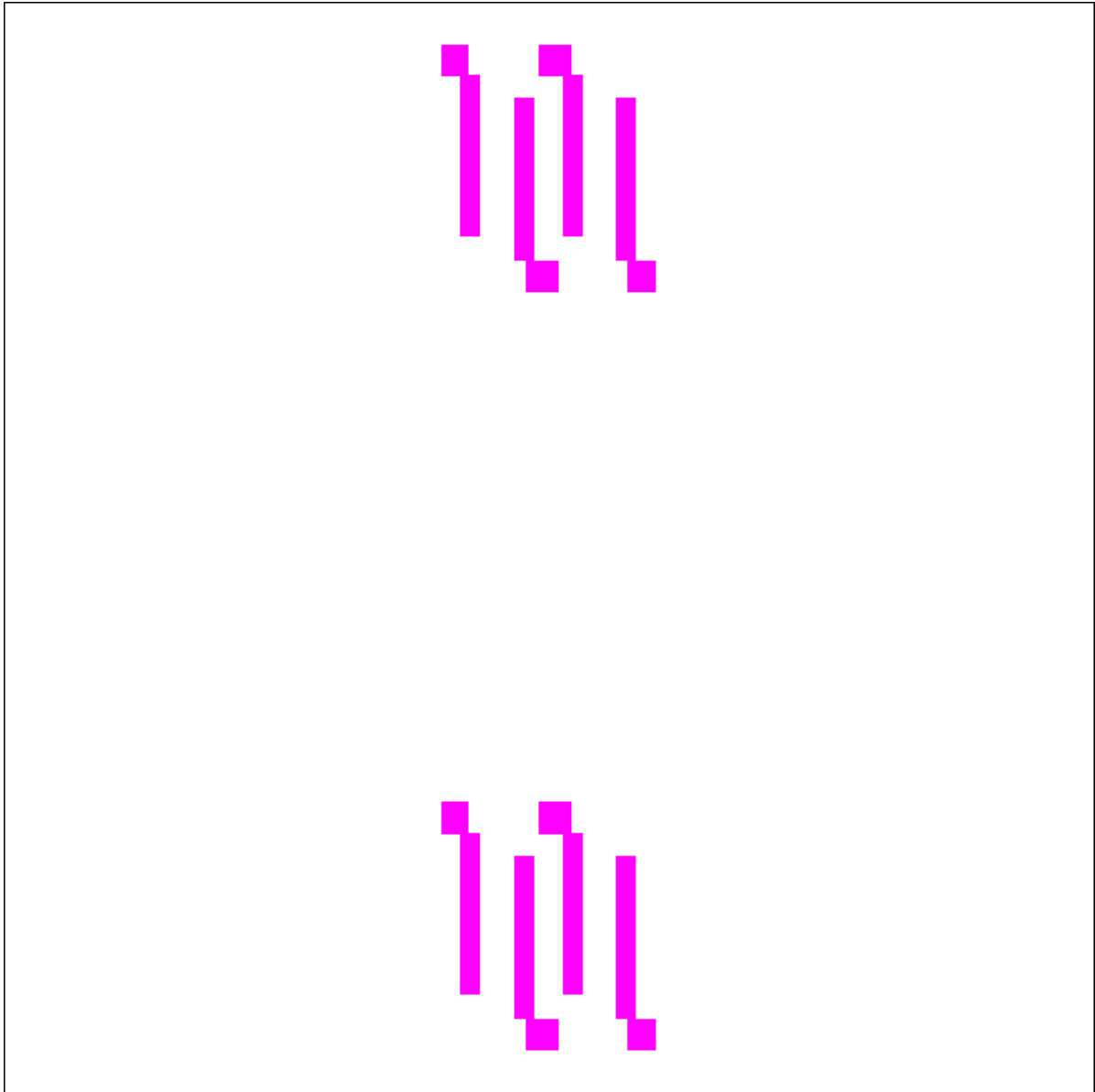


Figure B.2: Image used in Epson Print CD for top electrode

# Bibliography

- [1] J. Perelaer and U. S. Schubert, *8.07 - Ink-Jet Printing of Functional Polymers for Advanced Applications*. Amsterdam: Elsevier, 2012, pp. 147–175.
- [2] G.-K. Lau and M. Shrestha, “Ink-jet printing of micro-electro-mechanical systems (mems),” *Micromachines*, vol. 8, no. 6, 2017.
- [3] H. Rubaiyet Iftekharul, V. Rémy, G. Michel, V. Laurie, B. Patrick, and B. Xavier, “Inkjet printing of high molecular weight pvdf-trfe for flexible electronics,” *Flexible and Printed Electronics*, vol. 1, no. 1, p. 015001, 2016.
- [4] O. Pabst, J. Perelaer, E. Beckert, U. S. Schubert, R. Eberhardt, and A. Tünnermann, “All inkjet-printed piezoelectric polymer actuators: Characterization and applications for micropumps in lab-on-a-chip systems,” *Organic Electronics*, vol. 14, no. 12, pp. 3423–3429, 2013.
- [5] D. Thuau, K. Kallitsis, F. D. Dos Santos, and G. Hadziioannou, “All inkjet-printed piezoelectric electronic devices: energy generators, sensors and actuators,” *Journal of Materials Chemistry C*, vol. 5, no. 38, pp. 9963–9966, 2017.
- [6] Q. Liu, “Development of electrostrictive p(vdf-trfe-ctfe) terpolymer for inkjet printed electromechanical devices,” Thesis, 2016.
- [7] R. v. d. Nolle, “Production, design and control of p(vdf-trfe-ctfe) relaxor-ferroelectric actuators,” Thesis, 2017.
- [8] B. Curdin, G. Samuele, A. Hatem, and K. Gabor, “Inkjet printed multiwall carbon nanotube electrodes for dielectric elastomer actuators,” *Smart Materials and Structures*, vol. 25, no. 5, p. 055009, 2016.
- [9] S. Yuichi, F. Tomoaki, and A. Masatoshi, “Preparation of batio 3 thick films by inkjet printing on oxygen-plasma-modified substrates,” *Japanese Journal of Applied Physics*, vol. 45, no. 9S, p. 7247, 2006.
- [10] L. Engel, K. R. V. Volkinburg, M. Ben-David, G. N. Washington, S. Krylov, and Y. Shacham-Diamand, “Fabrication of a self-sensing electroactive polymer bimorph actuator based on polyvinylidene fluoride and its electrostrictive terpolymer,” in *SPIE Smart Structures and Materials + Nondestructive Evaluation and Health Monitoring*, vol. 9798. SPIE, Conference Proceedings, p. 11.
- [11] K. A. Schroder, *Mechanisms of photonic curing™: Processing high temperature films on low temperature substrates*, 2011, vol. 2.
- [12] 2017, ”Data Sheet: CI-004”. [Online]. Available: [http://intrinsicmaterials.com/wp-content/uploads/2018/04/CI-004\\_Data\\_Sheet\\_2017\\_v1.3.pdf](http://intrinsicmaterials.com/wp-content/uploads/2018/04/CI-004_Data_Sheet_2017_v1.3.pdf)
- [13] A. Hunt, M. Freriks, L. Sasso, P. Mohajerin Esfahani, and H. Hosseinnia, “Ipmc kirigami: A distributed actuation concept,” 07 2018, pp. 1–6.